ФИЗИКА ЭЛЕМЕНТАРНЫХ ЧАСТИЦ И АТОМНОГО ЯДРА
2011. Т. 42. ВЫП. 1

PROCESSES WITH HEAVY-ION COLLISIONS

A. B. Arbuzov [a], *V. V. Bytev* [a], *E. A. Kuraev* [a],
E. Tomasi-Gustafsson [b], *Yu. M. Bystritskiy* [a]

[a] Joint Institute for Nuclear Research, Dubna

[b] Institut de Physique Nucléaire, Orsay, France

ФИЗИКА ЭЛЕМЕНТАРНЫХ ЧАСТИЦ И АТОМНОГО ЯДРА
2011. Т. 42. ВЫП. 1

PROCESSES WITH HEAVY-ION COLLISIONS

A. B. Arbuzov [a], *V. V. Bytev* [a], *E. A. Kuraev* [a],
E. Tomasi-Gustafsson [b], *Yu. M. Bystritskiy* [a]

[a] Joint Institute for Nuclear Research, Dubna

[b] Institut de Physique Nucléaire, Orsay, France

Some Coulomb effects in heavy-ion collisions are considered. Among them are the process of muon- and lepton-pair creation, Coulomb and unitary corrections, statistics of multiple pair production. Effects of multiple photon exchange in process of lepton pair production by linearly polarized photon on nuclei are considered. This process is used for measuring the polarization of initial photon. Relativistic muon energy loss due to the light lepton pair production in the Coulomb field are calculated. Also we consider the effects of multiple photon exchange in elastic lepton scattering on unscreened atomic field and discuss the possible experimental testing.

Рассмотрены эффекты кулоновских поправок к столкновениям тяжелых ионов. В частности, изучено рождение мюонных и электронных пар, кулоновские и унитарные поправки, статистика множественного рождения лептонных пар. Рассчитаны поправки от множественного обмена виртуальными фотонами в процессе образования лептонных пар при рассеянии линейно поляризованного фотона на ядре, а также при рассеянии лептона на ядре. Этот процесс используется для мобильного определения степени линейной поляризации фотона. Изучены потери релятивистского мюона на образование лептонных пар в кулоновском поле, создаваемом ядрами атомов мишени.

PACS: 12.15.Lk; 12.20.-m; 12.20.Ds

To the blessed memory of Teachers Alexandr Ilich Akhiezer, Sergej Semenovich Sannikov, and Vladimir Naumovich Gribov

1. INTRODUCTION

In this review, several processes involving heavy-ion collisions are considered. In the beginning the semiclassical approach to the dynamics of pair creation is investigated. Then we put some expressions for pair production by polarized photon on ions with a charge Z, sufficiently large, so that higher orders of expansion on the parameter $Z\alpha$ become important. The case of screened nuclei is considered as well.

Also in Sec. 2 we consider the process of multiple lepton pair creation in the collisions of two heavy ions. All leading terms with respect to the parameter $Z\alpha$ are taken into account, including the exchange between ions and the screening effects, as well. We confirm the result obtained in quasi-classical approximation concerning the Poisson distribution in the coordinate space, for an inclusive experiment.

The problem of energy loss by the fast muon colliding with heavy nuclei is elaborated at the end of Sec. 2. It is shown that the main mechanism is the electron–positron pair production. At the end of this paper the interesting problem of measuring the deviation from the Rutherford formulae due to multiple photon exchanges is also discussed.

Throughout our paper we use the next designations: CC — Coulomb corrections; EPA — equivalent photon approximation; FD — Feynman diagram; LBL — light by light; LLA — leading logarithmic approximation; QED — quantum electrodynamics; RC — radiative corrections.

2. PROCESSES WITH HEAVY-ION COLLISIONS

2.1. Exclusive and Inclusive Muon Pair Production in Collisions of Relativistic Nuclei. Lepton pair production in ultrarelativistic nuclear collisions [10] were discussed in numerous papers (see [11] for a review and references therein). For the RHIC and LHC colliders the charge numbers of nuclei $Z_1 = Z_2 \equiv Z$ and their Lorentz factors $\gamma_1 = \gamma_2 \equiv \gamma$ are given in Table 1.

Table 1. **Colliders and cross sections for the lepton pair production**

Collider	Z	γ	$\sigma_B^{e^+e^-}$, kb	$\sigma_B^{\mu^+\mu^-}$, b
RHIC, Au–Au	79	108	36.0	0.23
LHC, Pb–Pb	82	3000	227	2.6
LHC, Ar–Ar	18	3400	0.554	0.0082

Below we will consider only 2γ mechanism of pair creation (Fig. 1). Bremsstrahlung mechanism, as well as the interference of corresponding amplitudes with 2γ contribution in fragmentation region of nuclei, is not considered here.

The cross section of one e^+e^--pair production in Born approximation, described by the Feynman diagram of Fig. 1, was obtained many years ago [5, 6]. Since the Born cross section $\sigma_B^{e^+e^-}$

$$\sigma_B^{e^+e^-} = \sigma_0(L^3 - 2.2L^2 + 3.8L - 1.63), \quad \sigma_0 = \frac{28}{27\pi}\frac{(z_1 z_2 \alpha^2)^2}{m_l^2},$$
$$L = \ln \gamma_1\gamma_2, \quad \gamma_i = \frac{E_i}{M_i}, \quad l = e, \mu \tag{2.1}$$

is huge (see Table 1), the e^+e^--pair production can be a serious background for many experiments. It is also an important issue for the beam lifetime and luminosity of these colliders [12]. It means that various corrections to the Born cross section, as well as the cross section for n-pair production, are of great importance. At present, there are a lot of controversial and incorrect statements in papers devoted to this subject. The corresponding references and critical remarks can be found in [11, 13, 37].

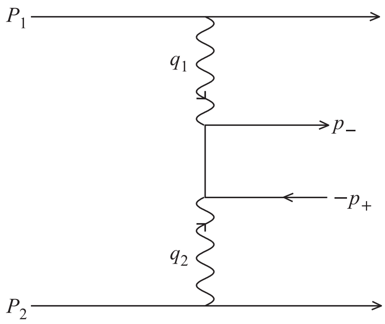

Fig. 1. The Feynman diagram for the 2γ lepton pair production mechanism in the Born approximation

Since the parameter $Z\alpha$ may be not small ($Z\alpha \approx 0.6$ for Au–Au and Pb–Pb collisions), the whole series in $Z\alpha$ has to be summed in order to obtain the cross section with sufficient accuracy. The exact cross section for one-pair production σ_1 can be split in the form

$$\sigma_1 = \sigma_B + \sigma_{\text{Coul}} + \sigma_{\text{unit}}, \tag{2.2}$$

where two different types of corrections need to be distinguished. The Coulomb correction σ_{Coul} corresponds to multiphoton exchange of the produced $e^\pm$ with the nuclei (Fig. 2); it was calculated in [13]. The unitary correction σ_{unit} corresponds to the exchange of light-by-light blocks between nuclei (Fig. 3); it was calculated in [37]. It was found in [13, 37] that the Coulomb corrections are large, while the unitary corrections are small (see Table 2). These results were confirmed recently in [14] by a direct summation of the Feynman diagrams.

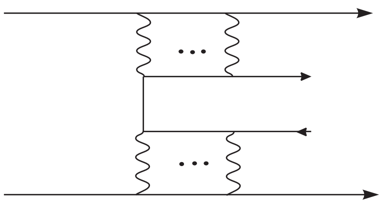

Fig. 2. The Feynman diargam for the Coulomb correction

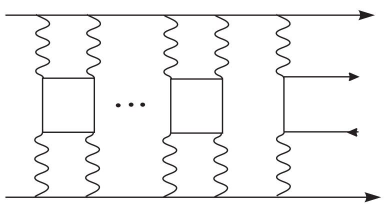

Fig. 3. The Feynman diagram for the unitary correction

Table 2. **Coulomb and unitary corrections to the e^+e^--pair production**

Collider	$\sigma_{\text{Coul}}/\sigma_B$, %	$\sigma_{\text{unit}}/\sigma_B$, %
RHIC, Au–Au	–10	–5.1
LHC, Pb–Pb	–9.4	–4.1

2.1.1. Born Cross Section for One $\mu^+\mu^-$-Pair Production in EPA. The production of one $\mu^+\mu^-$ pair

$$Z_1 + Z_2 \to Z_1 + Z_2 + \mu^+\mu^- \tag{2.3}$$

in the Born approximation is described by the Feynman diagram of Fig. 1.

When two nuclei with charges $Z_1 e$ and $Z_2 e$ and 4-momenta P_1 and P_2 collide with each other, they emit equivalent (virtual) photons with the 4-momenta q_1, q_2, energies ω_1, ω_2 and their virtualities $Q_1^2 = -q_1^2$, $Q_2^2 = -q_2^2$. Upon fusion, these photons produce a $\mu^+\mu^-$ pair with the total four-momentum $q_1 + q_2$ and the invariant mass squared $W^2 = (q_1 + q_2)^2$. Besides this, we denote

$$(P_1 + P_2)^2 = 4E^2 = 4M^2\,\gamma^2, \quad \alpha \approx 1/137.$$

The Born cross section of the process (2.3) can be calculated to a good accuracy using the EPA in the improved variant (presented, for example, in [7]). Let the numbers of equivalent photons be dn_1 and dn_2. The most important contribution to the production cross section stems from photons with very small virtualities $Q_i^2 \ll \mu^2$, where μ is the muon mass. Therefore, to a good approximation, the photons move in opposite directions, and $W^2 \approx 4\,\omega_1\,\omega_2$. In this very region the Born differential cross section $d\sigma_B$ for the process considered is related to the cross section $\sigma_{\gamma\gamma}$ for the process with real photons, $\gamma\gamma \to \mu^+\mu^-$, by the equation

$$d\sigma_B = dn_1\, dn_2\, d\sigma_{\gamma\gamma}(W^2). \tag{2.4}$$

The number of equivalent photons are (see Eq. (D.4) in [7])

$$dn_i(\omega_i, Q_i^2) = \frac{Z_i^2 \alpha}{\pi} \left(1 - \frac{\omega_i}{E_i}\right) \frac{d\omega_i}{\omega_i} \left(1 - \frac{Q_{i\,\min}^2}{Q_i^2}\right) F^2(Q_i^2)\, \frac{dQ_i^2}{Q_i^2}, \tag{2.5}$$

where

$$Q_i^2 \geqslant Q_{i\,\min}^2 = \frac{\omega_i^2}{\gamma^2} \tag{2.6}$$

and $F(Q^2)$ is the electromagnetic form factor of the nucleus. It is important that the integral over Q^2 converges rapidly for $Q^2 > 1/R^2$, where

$$R = 1.2\, A^{1/3}\ \text{fm} \tag{2.7}$$

is the radius of the nucleus with $A \approx M/m_p$ the number of nucleons ($R \approx 7$ fm, $1/R \approx 28$ MeV for Au and Pb). Since $Q_{\min}^2 \lesssim 1/R^2$, the main contribution to the cross section is given by virtual photons with energies

$$\omega_i \lesssim \gamma/R. \tag{2.8}$$

Therefore, we can use the spectrum of equivalent photons (neglecting terms proportional to ω_i/E_i) given by

$$dn_i(\omega_i, Q_i^2) = \frac{Z_i^2\alpha}{\pi}\,\frac{d\omega_i}{\omega_i}\,\left(1 - \frac{\omega_i^2}{\gamma^2 Q_i^2}\right)\,F^2(Q_i^2)\,\frac{dQ_i^2}{Q_i^2}. \tag{2.9}$$

After the transformation

$$\frac{d\omega_1}{\omega_1}\,\frac{d\omega_2}{\omega_2} = \frac{d\omega_1}{\omega_1}\,\frac{dW^2}{W^2}, \tag{2.10}$$

we cast the cross section in the form

$$d\sigma_B = \frac{Z_1^2\,Z_2^2\alpha^2}{\pi^2}\,\frac{d\omega_1}{\omega_1}\left(1 - \frac{\omega_1^2}{\gamma^2 Q_1^2}\right)F^2(Q_1^2)\,\frac{dQ_1^2}{Q_1^2}\times$$
$$\times\left(1 - \frac{\omega_2^2}{\gamma^2 Q_2^2}\right)\,F^2(Q_2^2)\,\frac{dQ_2^2}{Q_2^2}\,\frac{dW^2}{W^2}\,\sigma_{\gamma\gamma}(W^2),$$

where $\omega_2 \approx W^2/(4\omega_1)$.

2.1.2. Leading Logarithmic Approximation. Before using the above calculation scheme, it is instructive to present a rougher but simpler approximation — the so-called LLA. In the LLA, the equivalent photon spectrum as a function of photon energy $dn_i(\omega_i)$ is obtained after integrating $dn_i(\omega_i, Q_i^2)$ over Q_i^2 in the region between

$$Q_{i\ \min}^2 \leqslant Q_i^2 \lesssim 1/R^2, \tag{2.11}$$

which leads to

$$dn_i(\omega_i) \approx \frac{Z_i^2\alpha}{\pi}\,\ln\frac{\gamma^2}{(R\omega_i)^2}\,\frac{d\omega_i}{\omega_i}. \tag{2.12}$$

The restriction $Q_{i\ \min}^2 \lesssim 1/R^2$ corresponds to the integration interval

$$a = \frac{W^2R}{4\gamma} \lesssim \omega_1 \lesssim b = \frac{\gamma}{R}, \tag{2.13}$$

which gives

$$\sigma_B^{\mathrm{LLA}} = \frac{Z_1^2Z_2^2\alpha^2}{\pi^2}\int\limits_{4\mu^2}^{\infty}\frac{dW^2}{W^2}\,\sigma_{\gamma\gamma}(W^2)\int\limits_a^b\frac{d\omega_1}{\omega_1}\,\ln\frac{b^2}{\omega_1^2}\,\ln\frac{\omega_1^2}{a^2}. \tag{2.14}$$

Since $\sigma_{\gamma\gamma}(W^2) \approx (4\pi\alpha^2/W^2)\,\ln(W^2/\mu^2)$ for large values of $W \gg \mu$, the main contribution to the Born cross section comes from the region of small values of W near the threshold. Therefore, within logarithmic accuracy we replace W by some fixed value $W_0 \sim 2\mu$ in the lower bound a. After that the integral over W^2 gives

$$I = \int\limits_{4\mu^2}^{\infty} \frac{dW^2}{W^2}\, \sigma_{\gamma\gamma}(W^2) = \frac{14\pi\alpha^2}{9\mu^2} \tag{2.15}$$

and further integration over ω_1 leads to

$$\int\limits_a^b \frac{d\omega_1}{\omega_1}\, \ln\frac{b^2}{\omega_1^2}\, \ln\frac{\omega_1^2}{a^2} = \frac{2}{3}\, L^3, \tag{2.16}$$

where

$$L = \ln\frac{\gamma^2}{(W_0 R/2)^2}. \tag{2.17}$$

As a result, we obtain

$$\sigma_B^{\mathrm{LLA}} = \frac{28}{27\pi}\, \frac{(Z_1\alpha Z_2\alpha)^2}{\mu^2}\, L^3 \tag{2.18}$$

in accordance with the result of Landau & Lifshitz [5,6]. The accuracy of the LLA depends on the choice of the value for W_0. If we use for numerical estimations $W_0 = 3\mu$, then the accuracy of the LLA for the colliders discussed is about 15%.

The same result can be obtained in the framework of the impact-parameter-dependent representation, which will also be useful later. For this aim, we introduce the probability for muon pair production $P_B(\rho)$ in the collision of two nuclei at a fixed impact parameter ρ. For $\gamma \gg 1$, it is possible to consider the nuclei as sources of external fields and to calculate $P_B(\rho)$ analytically using the same approach as in [37]. The Born cross section σ_B can then be obtained by the integration of $P_B(\rho)$ over the impact parameter:

$$\sigma_B = \int P_B(\rho)\, d^2\rho. \tag{2.19}$$

We calculate this probability in the LLA, using Eq. (2.4) with

$$dn_i = \frac{Z_i^2\alpha}{\pi^2}\, \frac{d\omega_i}{\omega_i}\, \frac{d^2\rho_i}{\rho_i^2}, \quad \omega_i \ll \frac{\gamma}{R}, \;\; R \ll \rho_i \ll \frac{\gamma}{\omega_i}, \tag{2.20}$$

where ρ_i is the impact parameter of ith equivalent photon with respect to the ith nucleus. This allows us to write the above probability in the form

$$P_B(\rho) = \int dn_1\, dn_2\, \delta(\boldsymbol{\rho}_1 - \boldsymbol{\rho}_2 - \boldsymbol{\rho})\, \sigma_{\gamma\gamma}(W^2) = \frac{28}{9\pi^2}\, \frac{(Z_1\alpha Z_2\alpha)^2}{(\mu\rho)^2}\, \Phi(\rho). \tag{2.21}$$

Depending on the value of ρ, two different forms for $\Phi(\rho)$ need to be used:

$$\Phi(\rho) = \left(4\ln\frac{\gamma}{\mu\rho} + \ln\frac{\rho}{R}\right)\ln\frac{\rho}{R} \quad \text{for} \quad R \ll \rho \leqslant \frac{\gamma}{\mu}, \tag{2.22}$$

$$\Phi(\rho) = \left(\ln\frac{\gamma^2}{\mu^2\rho R}\right)^2 \qquad \text{for} \quad \frac{\gamma}{\mu} \leqslant \rho \ll \frac{\gamma^2}{\mu^2 R}. \tag{2.23}$$

Note that the function $\Phi(\rho)$ is continuous at $\rho = \gamma/\mu$ together with its first derivative. As expected, the integration of $P_B(\rho)$ over $\boldsymbol{\rho}$ in the region $R < \rho < \gamma^2/(\mu^2 R)$ gives back the result in (2.18) $\int(d^2\rho/\rho^2)\Phi(\rho) = (\pi/3)L^3$.

To prove (2.21)–(2.23), we make the transformation given in (2.10) together with the integration over W^2 according to (2.15). This gives

$$P_B(\rho) = \frac{14}{9\pi^3}\frac{(Z_1\alpha Z_2\alpha)^2}{\mu^2}\int\limits_{\mu^2R/\gamma}^{\gamma/R}\frac{d\omega_1}{\omega_1}\times$$
$$\times\int\frac{d^2\rho_1}{\rho_1^2(\boldsymbol{\rho}-\boldsymbol{\rho}_1)^2}\,\vartheta\left(\frac{\gamma}{\omega_1} - \rho_1\right)\vartheta\left(\frac{\gamma\omega_1}{\mu^2} - |\boldsymbol{\rho}-\boldsymbol{\rho}_1|\right),$$

where $\vartheta(x)$ is the step function. The main contribution to this integral is given by two regions: $R \ll \rho_1 \ll \rho$ and $R \ll |\boldsymbol{\rho}-\boldsymbol{\rho}_1| = \rho_2 \ll \rho$. Moreover, the two regions in the ω_1 integration with $\mu < \omega_1 < \gamma/R$ and $\mu^2R/\gamma < \omega_1 < \mu$ give the same contributions. As a result, we get

$$\Phi(\rho) = 2\,(J_1 + J_2)\,,$$
$$J_1 = \int\limits_{\mu}^{\gamma/R}\frac{d\omega_1}{\omega_1}\int\limits_{R}^{\rho}\frac{d\rho_1}{\rho_1}\,\vartheta\left(\frac{\gamma}{\omega_1} - \rho_1\right)\vartheta\left(\frac{\gamma\omega_1}{\mu^2} - \rho\right), \tag{2.24}$$
$$J_2 = \int\limits_{\mu}^{\gamma/R}\frac{d\omega_1}{\omega_1}\int\limits_{R}^{\rho}\frac{d\rho_2}{\rho_2}\,\vartheta\left(\frac{\gamma}{\omega_1} - \rho\right)\vartheta\left(\frac{\gamma\omega_1}{\mu^2} - \rho_2\right).$$

Next we consider the two regions of ρ.

In the region of relatively small impact parameters, $R \ll \rho \leqslant \gamma/\mu$, the second step function does not impose any limitations; therefore,

$$J_1 = \int\limits_{\mu}^{\gamma/\rho}\frac{d\omega_1}{\omega_1}\int\limits_{R}^{\rho}\frac{d\rho_1}{\rho_1} + \int\limits_{\gamma/\rho}^{\gamma/R}\frac{d\omega_1}{\omega_1}\int\limits_{R}^{\gamma/\omega_1}\frac{d\rho_1}{\rho_1} = \ln\frac{\gamma}{\mu\rho}\,\ln\frac{\rho}{R} + \frac{1}{2}\left(\ln\frac{\rho}{R}\right)^2,$$

$$J_2 = \int\limits_{\mu}^{\gamma/\rho}\frac{d\omega_1}{\omega_1}\int\limits_{R}^{\rho}\frac{d\rho_1}{\rho_1} = \ln\frac{\gamma}{\mu\rho}\,\ln\frac{\rho}{R}.$$

Summing up, we obtain (2.22). In the region of relatively large impact parameters, $\gamma/\mu \leqslant \rho \ll \gamma^2/(\mu^2 R)$, we have

$$J_1 = \int\limits_{\mu^2\rho/\gamma}^{\gamma/R} \frac{d\omega_1}{\omega_1} \int\limits_{R}^{\gamma/\omega_1} \frac{d\rho_1}{\rho_1} = \frac{1}{2}\left(\ln\frac{\gamma^2}{\mu^2 R\rho}\right)^2, \quad J_2 = 0;$$

therefore, the sum gives (2.23).

We compare Eqs. (2.21)–(2.23) for $\Phi(\rho)$ with the numerical calculations based on the exact matrix element calculated with the approach as outlined in [15]. We find good agreement for Pb–Pb collisions: the discrepancy is less than 10% at $\mu\rho > 10$ and less than 15% at $\mu\rho > 2\mu R = 7.55$.

2.1.3. More Refined Calculation. In the calculation below, for the form factor of the nucleus we use the simple approximation of a monopole form factor, which corresponds to an exponentially decreasing charge distribution, whose mean squared radius $\sqrt{\langle r^2\rangle}$ is adjusted to the experimental value:

$$F(Q^2) = \frac{1}{1+Q^2/\Lambda^2}, \quad \Lambda^2 = \frac{6}{\langle r^2\rangle}. \tag{2.25}$$

For lead and gold, the parameter is $\Lambda \approx 80$ MeV. This approximation of the form factor enables us to perform some calculations analytically, which otherwise could only be done numerically.

The equivalent photon spectrum $dn_i(\omega_i)$ is obtained after integrating $dn_i(\omega_i, Q_i^2)$ over Q_i^2 (the upper limit of this integration can be set to be equal to infinity in a good approximation, due to the fast convergence of the integral at $Q^2 > \Lambda^2$):

$$dn_i(\omega_i) = \frac{Z_i^2\alpha}{\pi} f\left(\frac{\omega_i}{\Lambda\gamma}\right)\frac{d\omega_i}{\omega_i}. \tag{2.26}$$

Here the function

$$f(x) = (1+2\,x^2)\,\ln\left(\frac{1}{x^2}+1\right) - 2 \tag{2.27}$$

is large for small values of x,

$$f(x) \approx \ln\frac{1}{x^2} - 2 = \ln\frac{1}{(\mathrm{e}x)^2} \ \text{ at } \ x \ll 1, \quad e = 2.71\ldots, \tag{2.28}$$

but drops very quickly for large x in accordance with Eq. (2.8):

$$f(x) < \frac{1}{6\,x^4} \ \text{ for } \ x > 1. \tag{2.29}$$

Finally, we obtain

$$\sigma_B = \frac{Z_1^2 Z_2^2 \alpha^2}{\pi^2} \int\limits_{4\mu^2}^{\infty} \frac{dW^2}{W^2}\, G(W^2)\, \sigma_{\gamma\gamma}(W^2) = \frac{(Z_1\alpha Z_2\alpha)^2}{\pi\mu^2}\, J(\gamma\Lambda/\mu), \qquad (2.30)$$

where

$$G(W^2) = \int\limits_{\omega_{\min}}^{\omega_{\max}} \frac{d\omega}{\omega}\, f\left(\frac{\omega}{\Lambda\gamma}\right)\, f\left(\frac{W^2}{4\Lambda\gamma\omega}\right). \qquad (2.31)$$

Since $\omega_i < E$ and $\omega_1\omega_2 \sim \mu^2$, we have $\omega_{\min} \sim \mu^2/E$ and $\omega_{\max} = E$. However, due to the fast decrease of $f(x)$ for $x > 1$, one can extend these limits up to $\omega_{\min} = 0$ and $\omega_{\max} = \infty$ without any lack of accuracy; therefore,

$$G(W^2) = 2 \int\limits_0^{\infty} f(x_1)\, f(x_2)\, dy, \quad x_{1,2} = \frac{W}{2\Lambda\gamma}\, \mathrm{e}^{\pm y}. \qquad (2.32)$$

A numerical evaluation of the integrals in Eqs. (2.30) and (2.31) yields the function $J(\gamma\Lambda/\mu)$ presented in Fig. 4.

Corrections to the photon spectrum are represented by terms in Eqs. (2.4) and (2.9) of the order of Q_i^2/W^2 (see Eqs. (E.1) in [7]), which are dropped before the integration over Q_i^2 is done. After the integration with weight $1/Q_i^2$, the relative value of these corrections becomes of the order of

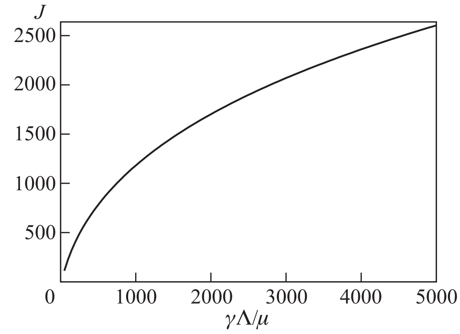

Fig. 4. The function $J(\gamma\Lambda/\mu)$ from Eq. (2.30)

$$\eta_1 = \frac{\Lambda^2}{W^2 L}. \qquad (2.33)$$

Thus, for the collisions considered here one can estimate the accuracy of the calculations on the level $\eta_1 \sim 5\%$. Another test of accuracy of the approach used is given in Subsubsec. 2.1.7.

Note that in the LLA the function $G(W^2)$ is just

$$G^{\mathrm{LLA}}(W^2) = \frac{2}{3}\left[\ln \frac{\gamma^2}{(eW/2\Lambda)^2}\right]^3 \approx \frac{2}{3}\left[\ln \frac{\gamma^2}{(WR/2)^2}\right]^3 \qquad (2.34)$$

in accordance with Eq. (2.16) (taking into account that $\Lambda/e \approx 1/R$, $e = 2,718\ldots$).

2.1.4. Coulomb and Unitary Corrections. For electron–positron pair production the relative value of Coulomb corrections and the unitarity ones are summarized in Table 2. The Coulomb corrections can be estimated as [13]

$$\frac{\sigma_{\text{Coul}}}{\sigma_0} = 6f(z\alpha)(L^2 - 5.5), \quad f(x) = x^2 \sum_1^\infty \frac{1}{n(n^2 + x^2)}. \tag{2.35}$$

The formulae for unitarity corrections are discussed below (see also [37]).

Consider now production of the $\mu^+\mu^-$ pairs. Due to the restriction of the transverse momenta of additionally exchanged photons to the range below $1/R$, the effective parameter of the perturbation series is not $(Z\alpha)^2$ but $(Z\alpha)^2/(R\mu)^2$. In addition, the contribution of the additional photons is suppressed by a logarithmic factor. Indeed, the cross section for two-photon production mechanism is proportional to L^3, while the cross section for the multiple-photon production mechanism is proportional only to L^2. Therefore, the real parameter describing the suppression of the Coulomb correction is of the order of

$$\eta_2 = \frac{(Z\alpha)^2}{(R\mu)^2 L}, \tag{2.36}$$

which corresponds to Coulomb corrections. This quantity is of order 0.01.

The unitary correction σ_{unit} to the one-muon-pair production corresponds to the exchange of light-by-light blocks between the two nuclei (Fig. 3). We start with a more general process — the production of one $\mu^+\mu^-$ pair and n electron–positron pairs ($n \geqslant 0$) in a collision of two ultrarelativistic nuclei

$$Z_1 + Z_2 \to Z_1 + Z_2 + \mu^+\mu^- + n\,(e^+e^-) \tag{2.37}$$

with the unitary corrections, which correspond to the exchange of the blocks of light-by-light scattering via the virtual lepton loops. The corresponding cross section $d\sigma_{1+n}$ can be calculated by a simple generalization of the results obtained in [14] for the n-pair process without muon pair production: $Z_1 + Z_2 \to Z_1 + Z_2 + n\,(e^+e^-)$. This multiple-pair-production process was studied in a number of papers, see [11] for a review. It was found that the probability is to a good approximation given by a Poisson distribution with the deviations found to be small. Indeed, it is not difficult to show that the basic equations for the latter process should be modified and the additional factor

$$\tilde{B}^\mu(\boldsymbol{\rho}, \mathbf{r}_{n+1}) \exp\left\{-L\left[\frac{A^\mu(\rho)}{2} + i\varphi^\mu(\rho)\right]\right\} \tag{2.38}$$

appears under the integral, where $L = \ln(\gamma_1\gamma_2)$ and the functions $\tilde{B}^\mu$, A^μ and φ^μ are the same as the functions given in Subsubsec. 2.4.3 but with the replacement of electrons by muons. As a result, Eq. (31) of [14] is replaced by

$$\frac{d\sigma_{1+n}}{d^2\rho} = LA_1^{\mu}(\rho)\,\frac{[LA_1(\rho)]^n}{n!}\,\mathrm{e}^{-LA_1^{\mu}(\rho)-LA_1(\rho)}, \tag{2.39}$$

where $LA_1^{\mu}(\rho) \approx P_B(\rho)$ is the probability of one-muon-pair production in the Born approximation. In the region of interest, $\rho > 2R$, the function $A_1^{\mu}(\rho)$ is small,

$$LA_1^{\mu}(\rho) \ll 1, \ \ A_1^{\mu}(\rho) \ll A_1(\rho); \tag{2.40}$$

therefore, we can rewrite (2.39) in the simpler form

$$\frac{d\sigma_{1+n}}{d^2\rho} = P_{1+n}(\rho), \ \ P_{1+n}(\rho) = P_B(\rho)\,\frac{[\bar{n}_e(\rho)]^n}{n!}\,\mathrm{e}^{-\bar{n}_e(\rho)}, \tag{2.41}$$

where $\bar{n}_e(\rho) = LA_1(\rho)$ is the average number of e^+e^- pairs produced in collisions of the two nuclei at a given impact parameter ρ. The result that the probabilities for the different processes factorize is due to the independence of the individual processes. For a general discussion of the validity of this factorization together with possible violations, we refer to [15].

In particular, we get the cross section for the exclusive one $\mu^+\mu^-$-pair production, including the unitary correction as

$$\sigma_{1+0} = \int P_B(\rho)\,\mathrm{e}^{-\bar{n}_e(\rho)}\,d^2\rho. \tag{2.42}$$

This expression can be rewritten in the form

$$\sigma_{1+0} = \sigma_B + \sigma_{\text{unit}}, \tag{2.43}$$

where σ_B is the Born cross section defined in (2.19) and

$$\sigma_{\text{unit}} = -\int \left[1 - \mathrm{e}^{-\bar{n}_e(\rho)}\right]\, P_B(\rho)\, d^2\rho \tag{2.44}$$

corresponds to the unitary correction for the one-muon-pair production.

A rough estimation of σ_{unit} can be done as follows. The main contribution to σ_{unit} comes from the region

$$R \ll \rho \ll \frac{1}{m_e}, \tag{2.45}$$

in which the function $\bar{n}_e(\rho) \approx \bar{n}_e(2R)$ and the integral (2.44) can be calculated in LLA. It gives

$$\sigma_{\text{unit}} \sim -\frac{28}{27\pi}\frac{(Z_1\alpha Z_2\alpha)^2}{\mu^2}\,\left[1 - \mathrm{e}^{-\bar{n}_e(2R)}\right]\, J_{\text{unit}}, \tag{2.46}$$

where

$$J_{\text{unit}} = 6 \int\limits_{2R}^{1/m_e} \Phi(\rho)\, \frac{d\rho}{\rho}. \tag{2.47}$$

As a result, we find $\sigma_{\text{unit}} \sim -1.2$ b for the Pb–Pb collisions at the LHC, which corresponds approximately to –5% of the Born cross section (see Table 2).

It is seen that unitary corrections are large; in other words, the exclusive production of one muon pair differs considerably from its Born value.

2.1.5. Inclusive Production of One $\mu^+\mu^-$ Pair. The experimental study of the exclusive muon-pair production seems to be a very difficult task. Indeed, this process requires that the muon pair should be registered without any electron–positron pair production, including $e^\pm$ emitted at very small angles. Otherwise, the corresponding cross section will be close to the Born cross section.

To prove this, let us consider the process (2.37), whose probability is given by Eq. (2.41). The corresponding cross section is

$$\sigma_{1+n} = \int P_{1+n}(\rho)\, d^2\rho. \tag{2.48}$$

It is clearly seen from this equation that, after summing up over all possible electron pairs, we obtain the Born cross section

$$\sum_{n=0}^{\infty} \sigma_{1+n} = \sigma_B. \tag{2.49}$$

Therefore, there is a very definite prediction: the inclusive muon-pair-production cross section coincides with the Born one. This direct consequence of calculations, which take into account strong field effects, may be easier to test experimentally than the prediction for cross sections of several e^+e^--pair production.

Let us discuss the relation of the cross sections obtained for the muon-pair production with the differential cross section of the e^+e^--pair production in the region of large transverse momenta for the $e^\pm$, for example, at $p_{\pm\perp} \gtrsim 100$ MeV. It is clear that for the e^+e^--pair production in this region, the situation is similar to the case considered for $\mu^+\mu^-$-pair production.

2.1.6. Two-Muon-Pair Production. The cross section of the process

$$Z_1 Z_2 \to Z_1 Z_2 + \mu^+\mu^-\mu^+\mu^- \tag{2.50}$$

can be calculated in lowest order in α according to

$$\sigma_2 = \frac{1}{2} \int \left[P_B(\rho)\right]^2 d^2\rho, \tag{2.51}$$

with the integration region $\rho \geqslant 2R$. But in this region the probability $P_B(\rho)$ is given to a good accuracy by Eqs. (2.23), (2.1.2). From this we get $\sigma_2 = 1.24$ mb for Pb–Pb collisions at the LHC.

2.1.7. Testing of EPA Spectrum Accuracy. To test the approach used in Subsubsec. 2.1.3, we consider the simpler case of the muon-pair production by a real photon with the energy ω off a nucleus

$$\gamma Z \to Z\mu^+\mu^-. \tag{2.52}$$

This cross section was calculated by Ivanov and Melnikov in [16] using the same expression (2.25) for the form factor of the nucleus and assuming $\Lambda^2/(2\mu)^2 \ll 1$. The corresponding formula for the Born contribution and the first Coulomb correction is

$$\sigma_{\gamma Z} = \frac{28}{9}\,\frac{Z^2\alpha^3}{\mu^2}\,(l - C_1 - C_2), \tag{2.53}$$

where

$$l = \ln\frac{2\omega\Lambda}{\mu^2} - \frac{57}{14}, \;\; C_1 = \frac{12}{35}\left(\frac{\Lambda}{2\mu}\right)^2, \;\; C_2 = 0.92(Z\alpha)^2\,C_1. \tag{2.54}$$

Therefore, the relative magnitude of the Coulomb correction is given by

$$\eta_2 = \frac{C_2}{l}, \tag{2.55}$$

which confirms the estimate in (2.36).

In the equivalent photon approximation, the cross section is given by

$$d\sigma_{\gamma Z}^{\mathrm{EPA}} = dn_2\,\sigma_{\gamma\gamma}(W^2), \tag{2.56}$$

which has the form

$$\sigma_{\gamma Z}^{\mathrm{EPA}} = \frac{Z^2\alpha}{\pi}\int\limits_{4\mu^2}^{\infty}\frac{dW^2}{W^2}\,f\left(\frac{W^2}{2\omega\Lambda}\right)\,\sigma_{\gamma\gamma}(W^2). \tag{2.57}$$

The main contribution to this integral is given by the region near the lower limit, where the argument of the function f is small and, therefore, f can be replaced by its approximate expression (2.28):

$$f\left(\frac{W^2}{2\omega\Lambda}\right) = 2\,\ln\frac{\omega\Lambda}{2\mu^2} - 2 - 2\,\ln\frac{W^2}{4\mu^2}. \tag{2.58}$$

After that the cross section can be calculated without difficulties as

$$\sigma_{\gamma Z}^{\mathrm{EPA}} = 2\,\frac{Z^2\alpha}{\pi}\left[\left(\ln\frac{\omega\Lambda}{2\mu^2} - 1\right)\,I - I_1\right] = \frac{28}{9}\,\frac{Z^2\alpha^3}{\mu^2}\,l, \tag{2.59}$$

where I is given by (2.15) and

$$I_1 = \int\limits_{4\mu^2}^{\infty} \frac{dW^2}{W^2}\,\sigma_{\gamma\gamma}(W^2)\,\ln\frac{W^2}{4\mu^2} = \frac{(43 - 28\ln 2)\,\pi\alpha^2}{9\mu^2}. \qquad (2.60)$$

Comparing this expression with the one of (2.53), we find that those terms which are omitted in the EPA have a relative magnitude of the order of

$$\eta_1 = \frac{C_1}{l}; \qquad (2.61)$$

this expression confirms the estimation (2.33).

2.2. Electron–Positron Pair Production by Linearly Polarized Photon in the Nuclear Field. Studies of a pair-creation process started in the celebrated papers of 1953–1969 and continue to attract the attention up to now [17–19,40,41]. Main interest nowadays is the use of this process as a polarimeter [31]. Really, it has rather a large cross section and the polarization effects can reach 14% [3,42]. Two different mechanisms of pair creation must be taken into account: the Bethe–Heitler one, when the pair is produced in collision of two photons — one real and the other virtual, and the bremsstrahlung mechanism, when a pair is created by a single virtual photon. It was shown in the fundamental papers by E. Haug [20] that at photon energies exceeding 50 MeV in the target laboratory frame the contribution of the bremsstrahlung mechanism, as well as the interference of the corresponding amplitude with two-photon ones, does not exceed 5% and decreases with further photon energy growth. Taking into account the lowest order RC does not change the situation. In the case of target such as proton or light nuclei, the main contribution to RC is connected with final-state interaction between pair components. The two-virtual-photon exchange between a particle and nuclei amplitude does not interfere with the Born amplitude as they have different signatures. Pure two-photon-exchange amplitude contribution does not contain any enhancement factors, such as «large logarithms» of ratio of photon energy ω to lepton mass m, and has order α^2. It can be neglected compared with contribution of order α/π coming from interference of Born amplitude with 1-loop ones connected with lepton-pair interaction.

The situation changes when one considers the pair creation on heavy nuclei with the charge parameter $\nu = Z\alpha$ being not too small. The main contribution arises from a many-photon exchange mechanism between a pair component with nuclei.

The total cross section of pair-creation process by photon on nuclei of charge Z

$$\begin{gathered} \gamma(k) + Y(P,Z) \to e^-(p_1) + e^+(p_2) + Y(P',Z), \quad q = P - P', \\ s = 2Pk = 2M\omega, \quad P^2 = (P')^2 = M^2, \quad p_\pm^2 = m^2, \quad |q^2| \ll s, \end{gathered} \qquad (2.62)$$

for unpolarized photon is [1,41]

$$\sigma = \frac{28}{9}\frac{Z^2\alpha^3}{m^2}\left[\ln\frac{2\omega}{m} - \frac{109}{42} - f(z\alpha)\right], \tag{2.63}$$

and $f(x)$ is given in Eq. (2.35). This result has recently been reproduced in an informative paper by Ivanov and Melnikov [16], where the differential cross section was considered as well.

Direction of e^+ and e^- emittance correlates with the degree and direction of photon linear polarization, and so this process can serve as a polarimetric reaction for the measuring linear polarization of high-energy photons at the present beams in the region of photons. At the present time, experimental tasks request measurements of linear polarization of photon beams in the region of photon energy up to 1–2 GeV with accuracy near 1% or better.

The considered process was discussed in detail in the works mentioned above. Calculations in these works were carried out on the basis of wave functions of the final electron and positron in the external screened Coulomb field in the Furry–Sommerfeld–Maue approximation. This approximation is valid for high energy of produced particles, $m/\epsilon_{1,2} \ll 1$, and for small emitting angles $\theta_{1,2} \sim m/\epsilon_{1,2} \approx 10^{-3}$; $\epsilon_{1,2}$ is the energy of electron and positron, and m is the electron mass.

It is well known that the main contribution to the cross section of the considered process gives just the region of small emitting angles. In this subsection we use formalism of [9] to consider the case of linearly polarized photon.

First, we briefly sketch the relevant results of [16]. Sudakov's parametrization of 4-momenta is used below:

$$\begin{aligned} q &= \alpha_q k + \beta_q \tilde{P} + \mathbf{q}, \quad & q_i &= \alpha_i k + \beta_i \tilde{P} + \mathbf{q}_i, \\ p_1 &= x_1 k + y_1 \tilde{P} + \mathbf{p}_1, \quad & p_2 &= x_2 k + y_2 \tilde{P} + \mathbf{p}_2, \end{aligned} \tag{2.64}$$

where $\mathbf{a}$ is Euclidean two-dimensional vector $\mathbf{a} = (0, 0, a_x, a_y)$ orthogonal to photon 4-momentum $k = \omega(1, 1, 0, 0)$; $\tilde{P} = (M/2)(1, -1, 0, 0) = P - k(M^2/s)$ is the light-like 4-vector. The conservation law and on-mass-shell conditions lead to

$$\begin{aligned} & x_1 + x_2 = 1, \quad y_1 = \frac{c_1}{x_1 s}, \quad y_2 = \frac{c_2}{x_2 s}, \\ & c_l = \mathbf{p}_l^2 + m^2, \quad l = 1, 2; \quad \mathbf{q} = \mathbf{p}_1 + \mathbf{p}_2. \end{aligned} \tag{2.65}$$

The matrix element corresponding to N-photon exchange is

$$M_N = -i^N s \frac{8\pi^2 (eZ)^N}{N!} \int \prod_{i=1}^{N} \frac{d^2 q_i}{(2\pi)^2} \frac{F(q_i^2)}{\mathbf{q}_i^2} \delta^{(2)}\left(\sum q_i - q\right) J^{(N)}_{\gamma \to l\bar{l}}, \tag{2.66}$$

where $J^{(N)}_{\gamma l\bar{l}}$ is the impact factor which is rewritten in the simple form [2, 8, 16] with

$$J^{(N)}_{\gamma\to l\bar{l}}(\mathbf{p}_1,\mathbf{p}_2) = \bar{u}(p_1)\left[mS^{(N)}\hat{\epsilon} - 2x_1\mathbf{T}^{(N)}\boldsymbol{\epsilon} - \hat{T}^{(N)}\hat{\epsilon}\right]\frac{\hat{\tilde{P}}}{s}v(p_2). \qquad (2.67)$$

The quantities S, $\mathbf{T}$ obey the recurrent relations

$$S^{(N)}(\mathbf{p}_1,\mathbf{p}_2,\mathbf{q}_N) = \\ = S^{(N-1)}(\mathbf{p}_1,\mathbf{p}_2-\mathbf{q}_N) - S^{(N-1)}(\mathbf{p}_1-\mathbf{q}_N,\mathbf{p}_2), \quad N = 2,3,\ldots, \qquad (2.68)$$

and a similar expression for $\mathbf{T}^{(N)}$. The initial values, corresponding to the one-photon exchange, are

$$S^{(1)} = S^{(1)}(\mathbf{p}_1,\mathbf{p}_2) = \frac{1}{c_1} - \frac{1}{c_2}, \quad \mathbf{T}^{(1)} = \mathbf{T}^{(1)}(\mathbf{p}_1,\mathbf{p}_2) = \frac{\mathbf{p}_1}{c_1} + \frac{\mathbf{p}_2}{c_2}. \qquad (2.69)$$

Introducing the values

$$J^{(N)}_{S,\mathbf{T}} = \int\prod_1^N \frac{d^2q_iF(q_i^2)}{\mathbf{q}_i^2}[S^{(N)},\mathbf{T}^{(N)}]\,\delta^2\left(\sum q_i - q\right), \qquad (2.70)$$

and their Fourier transform

$$I^{(N)}_{S,\mathbf{T}}(\mathbf{r}_1,\mathbf{r}_2) = \int\frac{d^2\mathbf{p}_1\,d^2\mathbf{p}_2}{(2\pi)^2}\,\mathrm{e}^{i\mathbf{p}_1\mathbf{r}_1+i\mathbf{p}_2\mathbf{r}_2}J^{(N)}_{S,\mathbf{T}}, \qquad (2.71)$$

the recurrent relations can be written in the form

$$I^{(N)}_{S,\mathbf{T}}(\mathbf{r}_1,\mathbf{r}_2) = \pi I^{(N-1)}_{S,\mathbf{T}}(\mathbf{r}_1,\mathbf{r}_2)\Phi(\mathbf{r}_1,\mathbf{r}_2), \\ \Phi(\mathbf{r}_1,\mathbf{r}_2) = \frac{1}{\pi}\int(\mathrm{e}^{i\mathbf{q}\mathbf{r}_2} - \mathrm{e}^{i\mathbf{q}\mathbf{r}_1})\frac{d^2qF(q^2)}{\mathbf{q}^2}. \qquad (2.72)$$

In the Moliere approximation of atomic form factor in the Tomas–Fermi model (we use it below) the expression for the form factor is [22]

$$\frac{F(q^2)}{\mathbf{q}^2} = \frac{1-F_A}{\mathbf{q}^2} = \sum_1^3\frac{\alpha_i}{\mu_i^2+\mathbf{q}^2}, \qquad (2.73)$$

with $\alpha_1 = 0.1$; $\alpha_2 = 0.55$; $\alpha_3 = 0.35$ and $\mu_i = (mZ^{1/3})b_i$ with $b_1 = 6.0$; $b_2 = 1.2$; $b_3 = 0.3$. In this case the analytic expressions can be obtained:

$$\Phi(\mathbf{r}_1,\mathbf{r}_2) = 2\sum_1^3\alpha_i[K_0(\mu_i|r_2|) - K_0(\mu_i|r_1|)], \qquad (2.74)$$

with $K_{0,1}(z)$ modified Bessel functions. For the pure Coulomb potential $F(q^2) = 1$, we have $\Phi^c(\mathbf{r}_1, \mathbf{r}_2) = \ln(\mathbf{r}_1^2/\mathbf{r}_2^2)$.

The boundary of recurrent relations is

$$I_S^{(1)}(\mathbf{r}_1, \mathbf{r}_2) = \frac{1}{2} K_0(m|\mathbf{r}_1 - \mathbf{r}_2|)\, \Phi(\mathbf{r}_1, \mathbf{r}_2),$$
$$\mathbf{I}_T^{(1)}(\mathbf{r}_1, \mathbf{r}_2) = \frac{im(\mathbf{r}_1 - \mathbf{r}_2)}{2|\mathbf{r}_1 - \mathbf{r}_2|} K_1(m|\mathbf{r}_1 - \mathbf{r}_2|)\, \Phi(\mathbf{r}_1, \mathbf{r}_2). \tag{2.75}$$

The summation over the number of exchanged photons can be performed:

$$J_S(\mathbf{p}_1, \mathbf{p}_2) =$$
$$= \frac{i}{2\nu} \int \frac{d^2 r_1\, d^2 r_2}{(2\pi)^2}\, \mathrm{e}^{-i\mathbf{p}_1\mathbf{r}_1 - i\mathbf{p}_2\mathbf{r}_2} K_0(m|\mathbf{r}_1 - \mathbf{r}_2|)\nu[\mathrm{e}^{-i\nu\Phi(\mathbf{r}_1,\mathbf{r}_2)} - 1],$$
$$\mathbf{J}_T(\mathbf{p}_1, \mathbf{p}_2) = \tag{2.76}$$
$$= \frac{-1}{2\nu} \int \frac{d^2 r_1 d^2 r_2}{(2\pi)^2}\, \mathrm{e}^{-i\mathbf{p}_1\mathbf{r}_1 - i\mathbf{p}_2\mathbf{r}_2} \frac{m(\mathbf{r}_1 - \mathbf{r}_2)}{2|\mathbf{r}_1 - \mathbf{r}_2|} K_1(m|\mathbf{r}_1 - \mathbf{r}_2|)[\mathrm{e}^{-i\nu\Phi(\mathbf{r}_1,\mathbf{r}_2)} - 1].$$

The differential cross section has the form

$$d\sigma = \frac{2\alpha\nu^2}{\pi^2}[|\mathbf{J}_T|^2 + m^2|J_S|^2 - 4x(1-x)\mathbf{J}_T\boldsymbol{\epsilon}\mathbf{J}_T\boldsymbol{\epsilon}^*]\, dx\, d^2p_1 d^2p_2 =$$
$$= \frac{2\alpha\nu^2}{\pi^2}[W_{\text{unp}} + \xi_3 W_{\text{pol}} \cos(2\varphi)]\, dx\, d^2p_1\, d^2p_2, \tag{2.77}$$
$$\epsilon_i \epsilon_j^* \to \frac{1}{2}[I + \xi_1\sigma_1 + \xi_3\sigma_3]_{ij}, \quad i, j = x, y,$$

with the polarization degree of photon, described by means of $\xi_{1,3}$ being Stokes parameters, φ is the angle between the vector $\mathbf{J}_T$ and the direction of maximal polarization of photon (if we choose the x axis along the direction of maximal polarization of photon, we put $\xi_1 = 0; P = \xi_3$), and

$$W_{\text{unp}} = [x^2 + (1-x)^2]|\mathbf{J}_T|^2 + m^2|J_S|^2, \quad W_{\text{pol}} = -2x(1-x)|\mathbf{J}_T|^2. \tag{2.78}$$

For the screened potential (ignoring the experimental conditions of pair component definition), we use the expression for the phase given above. Performing the integration on pair momenta, we obtain

$$2\pi \frac{d\sigma}{dx_1 d\varphi_1} = \frac{2\alpha}{m^2} \int_0^{2\pi} \frac{d\varphi}{2\pi} \int_0^\infty dy_1 \int_0^\infty dy_2 (1 - \cos(\nu\varphi_{12}^c)) \times$$
$$\times [K_0^2(z) + [x_1^2 + (1-x_1)^2]K_1^2(z) - 2x_1(1-x_1)\xi_3 K_1^2(z)\cos(2\varphi)], \tag{2.79}$$
$$z = \sqrt{y_1 + y_2 - 2\sqrt{y_1 y_2}\cos\varphi_0},$$

with $\varphi_{12}^c = \Phi^c(\mathbf{r}_1, \mathbf{r}_2) = (1/2)\ln(y_1/y_2)$. The azimuthal angle φ_0 is the angle between the direction of maximal photon polarization and the plane containing the direction of initial photon and electron (positron) from the pair.

For the case of pure Coulomb potential, integration in (2.79) diverges and must be regularized. We leave here this academic problem. For the case of screened potential we obtain

$$2\pi \frac{d\sigma}{dx\, d\varphi_1} = \\ = \frac{2\alpha}{m^2}[a(\nu) + (x^2 + (1-x)^2)b(\nu) - 2x(1-x)\xi_3 \cos(2\varphi_1) b(\nu)]. \quad (2.80)$$

The ν dependence of coefficients $a(\nu), b(\nu)$ is shown in Fig. 5.

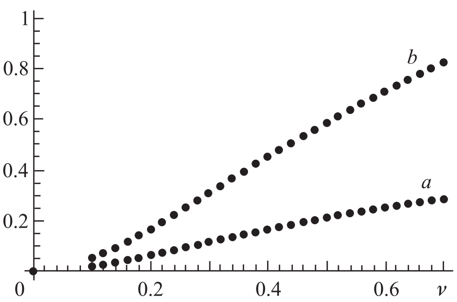

Fig. 5. The ν-dependence of coefficients a, b (see (2.79), (2.80))

Further we will consider the realistic case of nonzero momentum, transferred to nuclei $|\mathbf{q}|^2 \gg m^2$. For the pure Coulomb potential we have

$$\frac{d\sigma}{dx\, d\Omega_1\, d\Omega_2} = \frac{2\alpha\nu^2\omega^4}{\pi^2 m^2} \frac{x^2(1-x)^2}{(\mathbf{q}^2)^2} |\Gamma(1-i\nu)|^4 [W_u^c + \xi_3 W_p^c], \quad (2.81)$$

with

$$W_u^c = m^2[x^2 + (1-x)^2] \left| (2F_1 - F_2)\frac{\mathbf{p}_2}{c_2} + F_2 \frac{\mathbf{p}_1}{c_1} \right|^2 + \\ + \left| F_2 - F_1 + (2F_1 - F_2)\frac{m^2}{c_2} - F_2 \frac{m^2}{c_1} \right|^2, \quad (2.82)$$

$$W_p^c = -2x(1-x)m^2 \left[|2F_1 - F_2|^2 \frac{\mathbf{p}_2^2}{c_2^2} \cos(2\varphi_2) + \\ + |F_2|^2 \frac{\mathbf{p}_1^2}{c_1^2} \cos(2\varphi_1) + 2\,\mathrm{Re}\,(F_2^*(2F_1 - F_2)) \frac{|\mathbf{p}_2|}{c_2} \frac{|\mathbf{p}_1|}{c_1} \cos(\varphi_1 + \varphi_2) \right],$$

and $F_1 = F(i\nu, -i\nu; 1; z)$; $F_2 = (1 - i\nu)F(i\nu, 1 - i\nu; 2; z)$ are the Gauss hypergeometric functions, $z = 1 - \dfrac{m^2\mathbf{q}^2}{c_1 c_2}$, the value of transverse component of the pair is

$$|\mathbf{p}_1| = \omega x \theta_1; \quad |\mathbf{p}_2| = \omega(1-x)\theta_2,$$

$x, 1-x$ are the energy fractions of electron, positron. Here $\varphi_{1,2}$ are the azimuthal angles between the direction of maximal polarization of photon and the transverse component of electron and positron, $\theta_{1,2}$ are polar angles between photon direction and lepton pair component emission, $d\Omega_1\, d\Omega_2 = \theta_1\theta_2\, d\theta_1\, d\varphi_1\, d\theta_2\, d\varphi_2$ are phase volumes of the leptons.

In the case of small momentum transferred to nuclei $m^2 \ll \mathbf{q}^2 \ll \mathbf{p}_1^2 \approx \mathbf{p}_2^2$, we can put in (2.82) $z = 1$ and, using $F_1 = F_2 = |\Gamma(1 - i\nu)|^{-2}$, we reproduce the cross section in the Born approximation

$$\frac{d\sigma_B^c}{dx\, d\Omega_1\, d\Omega_2} = \frac{2\alpha^3 Z^2 \omega^4 x^2 (1-x)^2}{\pi^2 (\mathbf{q}^2)^2} \Bigg[m^2 (S^1)^2 + (x^2 + (1-x)^2)(\mathbf{T}^1)^2 - \\ - 2x(1-x)\xi_3 \left(\frac{\mathbf{p}_2^2}{c_2^2} \cos(2\varphi_2) + \frac{\mathbf{p}_1^2}{c_1^2} \cos(2\varphi_1) + \frac{|\mathbf{p}_2|}{c_2}\frac{|\mathbf{p}_1|}{c_1} \cos(\varphi_1 + \varphi_2) \right) \Bigg], \\ \vec{q}^2 > m^2. \tag{2.83}$$

We note that the quantity in square brackets in the rhs of (2.83) is proportional to $\mathbf{q}^2$ at small $\mathbf{q}^2$. The experimental restrictions connected with pair component detection can be imposed as a domain of variation of energy fractions and angles of electron and positron.

For the large transverse momentum of the pair component $p_1 = p_2 = p \gg m$, we have

$$\frac{d\sigma_B}{d\Omega_1\, d\Omega_2\, dx} = \frac{\alpha^3 \omega^4 (x(1-x))^2}{2\pi^2 p^6} \frac{1 - 2x(1-x)(1 + \xi_3 \cos(\varphi_1 + \varphi_2))}{\cos^2\left(\dfrac{\varphi_1 - \varphi_2}{2}\right)}, \\ \mathbf{q}^2 = 4p^2 \cos^2\left(\frac{\varphi_1 - \varphi_2}{2}\right) \gg m^2. \tag{2.84}$$

2.2.1. The Case of Screened Potential. In a more realistic case of the electromagnetic field of atom described above, we do not succeed in obtaining the result in a closed form. So we calculate the values $J_S, \mathbf{J}_T$ by expansion in series up to the terms of the first order of ν.

After this expansion we have for the scalar structure

$$J_S(\mathbf{p}_1, \mathbf{p}_2) = J_S^{(1)}(\mathbf{p}_1, \mathbf{p}_2) + \nu J_S^{(2)}(\mathbf{p}_1, \mathbf{p}_2), \\ J_S^{(1)}(\mathbf{p}_1, \mathbf{p}_2) = \left(\frac{1}{c_1} - \frac{1}{c_2}\right) \sum_{i=1}^{3} \frac{\alpha_i}{q^2 + \mu_1^2}, \tag{2.85}$$

$$J_S^{(2)} = i \sum_{i,j=1}^{3} \alpha_i \alpha_j \left[\left(\frac{1}{c_1} + \frac{1}{c_2} \right) B - T_2 - T_1 \right].$$

An analogous expression for the vector structure is

$$\mathbf{J}_T(\mathbf{p}_1, \mathbf{p}_2) = \mathbf{J}_T^{(1)}(\mathbf{p}_1, \mathbf{p}_2) + \nu \mathbf{J}_T^{(2)}(\mathbf{p}_1, \mathbf{p}_2),$$
$$\mathbf{J}_T^{(1)} = \left(\frac{\mathbf{p}_1}{c_1} + \frac{\mathbf{p}_2}{c_2} \right) \sum_{i.j=1}^{3} \frac{\alpha_i}{q^2 + \mu_1^2}, \tag{2.86}$$
$$\mathbf{J}_T^{(2)} = i \sum_{i,j=1}^{3} \alpha_i \alpha_j \left[\left(\frac{\mathbf{p}_1}{a_1} + \frac{\mathbf{p}_2}{a_2} \right) B - \mathbf{p}_1 T_1 + \mathbf{p}_2 T_2 + \mathbf{T}_1 - \mathbf{T}_2 \right].$$

The quantities B, T_l, and $\mathbf{T}_l$ are given in Subsubsec. 2.2.3.

The relevant contribution to the total cross section has the form

$$\frac{d\sigma}{dx\, d\Omega_1\, d\Omega_2} = \frac{d\sigma^{(1)}}{dx\, d\Omega_1\, d\Omega_2} + \frac{d\sigma^{(2)}}{dx\, d\Omega_1\, d\Omega_2}, \tag{2.87}$$

the first term is given above (see (2.83)) with replacement $S^{(1)} \to J_s^{(1)}$, $\mathbf{T}^{(1)} \to \mathbf{J}_T^{(1)}$. Writing $\mathbf{J}_T^{(2)}$ in the form $\mathbf{J}_T^{(2)} = A_1 \mathbf{p}_1 + A_2 \mathbf{p}_2$, the second term in (2.87) will be

$$\frac{d\sigma^{(2)}}{dx\, d\Omega_1\, d\Omega_2} = \frac{\alpha \nu^4}{4\pi^2} (x(1-x))^2 \omega^4 I_2, \tag{2.88}$$

with

$$I_2 = m^2 (J_S^{(2)})^2 + (x^2 + (1-x)^2)(\mathbf{J}_T^{(2)})^2 - 2\xi_3 x(1-x) \times$$
$$\times \left(A_1^2 \mathbf{p}_1^2 \cos(2\varphi_1) + A_2^2 \mathbf{p}_2^2 \cos(2\varphi_2) + 2 A_1 A_2 |\mathbf{p}_1||\mathbf{p}_2| \cos(\varphi_1 + \varphi_2) \right).$$

High-order contributions by $(Z\alpha)^n, n \gg 3$ can be expressed with iteration procedure. However, the analytic expression terms become more complicated. Nevertheless, the formulae given here provide the accuracy of order 1% for the case of pair photoproduction on light nuclei $Z\alpha < 0.3$.

2.2.2. Numerical Estimation. In famous papers by Bethe, Maximon and Olsen [17–19], the general theory of pair production and bremsstrahlung was built based on electron wave function in the Coulomb field. Part of these results was reproduced in a perturbation theory approach in [16]. Unfortunately, the expression for the differential cross sections which can be used in current experiments with specific cuts was rather poorly presented.

These results provide high accuracy, since they are valid in all orders of PT. Using them, the experimental restrictions can be put explicitly. In particular, the formula obtained above can describe the exclusive experiment with pairs photoproduction on a nuclei when both the electron and the positron are tagged.

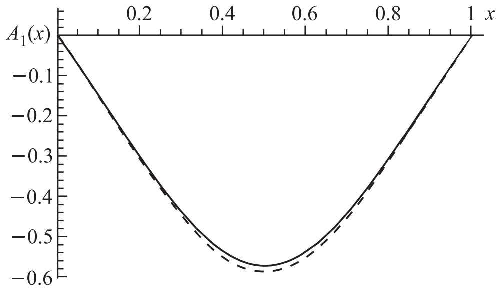

Fig. 6. Azimuthal asymmetry (see (2.80)); solid line — $\nu = 0.3$, dashed line — $\nu = 0.6$

In Fig. 6 the dependence of asymmetry defined as (see (2.80))

$$A(x, \xi_3) = \frac{d\sigma(\varphi_1 = 0) - d\sigma(\varphi_1 = \pi/2)}{d\sigma(\varphi_1 = 0) + d\sigma(\varphi_1 = \pi/2)} \tag{2.89}$$

is presented for $\xi_3 = 1$ as a function of electron energy fraction x.

Asymmetry calculated using formula (2.80) turns out to be rather large compared with the one obtained in [18] and reaches 40%. We should like to note that in [18] an emission restriction $\theta_\pm > 10^{-3}$ was put on. The main contribution, however, arises from small values of $p_{1,2} \ll m$, which is implied in our formula (2.80). Our result can be used in an experimental set-up with the magnetic field.

Asymmetry

$$A(x, p_1, p_2, \varphi_2, \xi_3) = \frac{d\sigma(\varphi_1 = 0, x, p_1, p_2, \varphi_2) - d\sigma(\varphi_1 = \pi/2, x, p_1, p_2, \varphi_2)}{d\sigma(\varphi_1 = 0, x, p_1, p_2, \varphi_2) + d\sigma(\varphi_1 = \pi/2, x, p_1, p_2, \varphi_2)}, \tag{2.90}$$
$$p_{1,2} = |\mathbf{p}_{1,2}|.$$

calculated by formulae with (2.83) at fixed values p_1, p_2 is drawn in Fig. 7. The lowest order correction to it for $\nu = 0.3$ is a quantity of order 10% of Born amplitude.

The differential distribution (2.83) is valid in the case of rather large values of transverse momenta of electron–positron pair and provides the possibility to apply the experimental detection details.

The cross section in the case of unpolarized particles is of the order

$$\sigma \approx 170 \text{ mb}, \quad Z = 79.$$

Accuracy of calculation is determined by the omitted terms

$$1 + \mathcal{O}\left(\frac{\mathbf{p}^2}{s}, \frac{\alpha}{\pi} \ln \frac{\mathbf{p}^2}{m^2}\right). \tag{2.91}$$

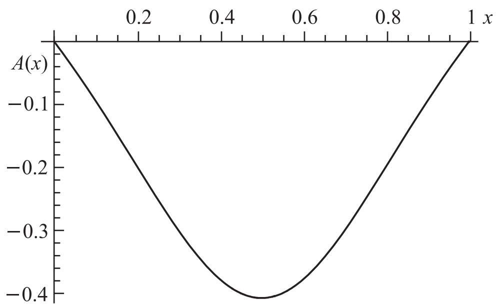

Fig. 7. Asymmetry in Born approach (see (2.84)); at fixed parameters: $p_1 = p_2 = 10$ MeV, $\xi_3 = 1$, $\varphi_2 = \pi/2$ (see (2.83))

The quantity of error is of the order of several percent. The last term corresponds to pair component of final-state interaction, which was not considered here.

This quantity does not depend on energy of the initial photon starting from rather high values of it ($\omega > 50$ MeV) in accordance with the results of [13].

We show besides (see Subsubsec. 2.2.3) that the effects of higher orders of expansion on the parameter $\nu = Z\alpha$ disappear in the case when transverse components of electron and positron momentum considerably exceed the electron mass. The screening effects in asymmetry disappear in this limit as well.

2.2.3. Explicit Calculation of Integrals. In the case of the screened potential the matrix element corresponding to two-photon exchange has the form

$$M^{(2)} = \frac{s(4\pi\alpha)^{5/2}Z^2}{4\pi} N_P \sum_{i,j=1}^{3} \alpha_i \alpha_j \bar{u}(p_2) \hat{R} \frac{\hat{P}}{s} v(p_1), \tag{2.92}$$

with

$$N_P = \frac{1}{s}\bar{u}(P')\hat{k}u(P), \quad \sum |N_P|^2 = 2, \tag{2.93}$$

and

$$\hat{R} = \int \frac{d^2k_1}{\pi} \frac{1}{\mathbf{k}_1^2 + \mu_i^2} \frac{1}{(\mathbf{q}-\mathbf{k}_1)^2 + \mu_j^2} \left[m\hat{e}S_2 + 2x\mathbf{T}_2\mathbf{e} + \hat{T}_2\hat{e} \right],$$
$$S_2 = \frac{1}{c_1} - \frac{1}{c_{1k}} + \frac{1}{c_2} - \frac{1}{c_{2k}}, \quad \mathbf{T}_2 = \frac{\mathbf{p}_1}{c_1} + \frac{\mathbf{k}_1 - \mathbf{p}_1}{c_{1k}} - \frac{\mathbf{p}_2}{c_2} - \frac{\mathbf{k}_1 - \mathbf{p}_2}{c_{2k}}, \tag{2.94}$$

where c_l was defined above, $c_{lk} = (\mathbf{k}_1 - \mathbf{p}_l)^2 + m^2$.

We need to calculate the integrals

$$
\begin{aligned}
B &= \int \frac{d^2k_1}{\pi(\mathbf{k}_1^2+\mu_i^2)((\mathbf{q}-\mathbf{k}_1)^2+\mu_j^2)},\\
(T_l,\mathbf{T}_l) &= \int \frac{d^2k_1(1,\mathbf{k}_1)}{\pi(\mathbf{k}_1^2+\mu_i^2)((\mathbf{q}-\mathbf{k}_1)^2+\mu_j^2)((\mathbf{p}_l-\mathbf{k}_1)^2+m^2)}.
\end{aligned}
\tag{2.95}
$$

Applying the Feynman joining procedure and performing the standard Feynman parameter integration, we obtain

$$
\begin{aligned}
T_l &= \int_0^1 dx\left\{-\frac{2A_1+B_1}{R\Delta}+\frac{2B_1}{R^{3/2}}L\right\}, \quad \Delta = A_1+B_1+C+1,\\
\mathbf{T}_l &= \int_0^1 dx\,\mathbf{p}_{xl}\left\{-\frac{2C_1+B_1}{R\Delta}+\frac{2C_1}{R^{3/2}}L\right\},\\
L &= \ln\frac{(B_1+2C_1+\sqrt{R})^2}{4C_1\Delta}, \quad R = B_1^2-4A_1C_1>0,
\end{aligned}
\tag{2.96}
$$

with

$$
\begin{gathered}
A_1 = -\mathbf{p}_{xl}^2, \quad \mathbf{p}_{xl} = x\mathbf{q}+(1-x)\mathbf{p}_l,\\
\Delta = (1-x)m^2+x\mu_j^2+x(1-x)(q-p_l)^2, \quad C_1=\mu_i^2,\\
B_1 = (1-x)(\mathbf{p}_l^2+m^2)+x(\mathbf{q}^2+\mu_j^2)-\mu_i^2.
\end{gathered}
\tag{2.97}
$$

In the kinematic region $m^2 \sim \mu_i^2 \ll \mathbf{q}^2 \ll \mathbf{p}_i^2 = \mathbf{p}_2^2 = \mathbf{p}^2$, we obtain

$$
B = \frac{2}{\mathbf{q}^2}\ln\frac{\mathbf{q}^2}{\mu_i\mu_j}, \;\; T_1 = T_2 = \frac{2}{\mathbf{p}^2\mathbf{q}^2}\ln\frac{\mathbf{q}^2}{\mu_i\mu_j}, \;\; \mathbf{T}_1 = \mathbf{T}_2 = \frac{\mathbf{q}}{\mathbf{p}^2\mathbf{q}^2}\ln\frac{\mathbf{p}^2}{\mu_j^2}. \tag{2.98}
$$

In this limit we have $S^{(2)} = \mathbf{T}^{(2)} = 0$. It can be shown that $S^{(n)} = \mathbf{T}^{(n)} = 0, n>2$ is fulfilled in this limit as well.

2.3. Production of e^+e^- Pairs to All Orders in $Z\alpha$ for Collisions of High-Energy Muons with Heavy Nuclei. The production of e^+e^- pairs in collisions of high-energy muons with nuclei and atoms is important for a number of problems [30, 32]. In particular, this process is dominant for energy losses of muons passing through matter. A precise knowledge of these losses is necessary for the construction of detectors and $\mu^+\mu^-$ colliders and an estimation of shielding at high-energy colliders.

In Born approximation, various cross sections for the process under discussion (A denotes an atom or a nucleus with charge number Z)

$$
\mu A \to \mu A\; e^+e^- \tag{2.99}
$$

have been calculated in [5, 6, 24, 25]. A recent short review on the muon energy loss at high energy can be found in Sec. 23.9 of [9]. Some useful approximate formulae and figures are given in [26].

In all the mentioned papers, effects of high-order corrections in the parameter

$$\nu = Z\alpha \approx \frac{Z}{137} \tag{2.100}$$

have not been taken into account. However, this parameter is of the order of 1 for heavy nuclei ($\nu = 0.6$ for Pb) and, therefore, the whole series in ν has to be summed to achieve an exact result for the process (2.99).

Let M_n be the amplitude of the discussed process with n exchanged photons (Fig. 8). We present the cross section in the form

$$\begin{gathered} d\sigma = d\sigma_B + d\sigma_{\rm Coul}, \\ d\sigma_B \propto |M_B|^2 = |M_1|^2, \\ d\sigma_{\rm Coul} \propto \left|\sum_{n=1}^{\infty} M_n\right|^2 - |M_1|^2, \end{gathered} \tag{2.101}$$

where $M_B = M_1$ denotes the Born amplitude. We call the CC the difference $d\sigma_{\rm Coul}$ between the exact result and the Born approximation.

Such a kind of CC is well known in the photoproduction of e^+e^- pairs on atoms (see [17, 27], § 32.2 of [1] and § 98 of [2]). In case of the total cross section, the corrections are negative and decrease the Born contribution by about 10% for Pb.

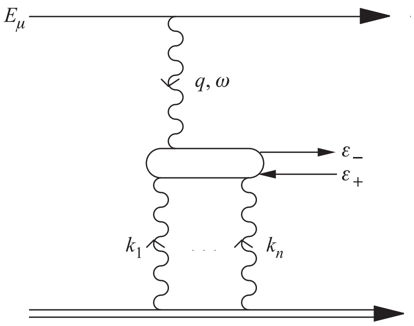

Fig. 8. Amplitude M_n with n exchanged photons for the reaction $\mu A \to \mu A\, e^+e^-$

In this subsection we calculate CC for the reaction (2.99), neglecting only terms of the order of

$$\frac{m_\mu^2}{E_\mu^2}, \quad \frac{m_e}{\varepsilon_\pm}. \tag{2.102}$$

Therefore, our results are valid for ultrarelativistic leptons. In (2.102) m_e and m_μ are the lepton masses, $\varepsilon_\pm$ and E_μ denote the lepton energies.

The discussed process for $\varepsilon_\pm \ll E_\mu$ has a close relation to $A'A \to A'Ae^+e^-$, where A' is a fast nucleus with relatively small charge $Z'\alpha \ll 1$ and A is a heavy atom or nucleus with $Z\alpha \sim 1$. The latter process was considered in [28] and [23], assuming that the lepton energies are much smaller than the energy of the projectile nucleus A'. In these papers the same complicated method has been used as in [17], which basically uses approximated relativistic wave functions of e^+ and e^- in the Coulomb field of the nucleus A.

Our approach is more simple and transparent. It is based on cross sections for the virtual process $\gamma^* A \to e^+e^- A$ (where γ^* denotes the virtual photon with 4-momentum squared $q^2 < 0$) which has recently been obtained in [16] by a direct summation of the corresponding Feynman diagrams. For $\varepsilon_\pm \ll E_\mu$ our Eqs. (2.115) and (2.125) coincide with Eqs. (38) and (39) of [28], respectively, while our Eq. (2.109) coincides with the corresponding equation of [23] only in the main logarithmic approximation. (It should be noted, however, that the results of [23] for the discussed process are also presented with logarithmic accuracy.)

2.3.1. Energy Distribution of e^+ and e^-. It is well known [9] that the cross section for the process (2.99), as well as for electroproduction, can be exactly written in terms of two structure functions or two cross sections $\sigma^T(\omega, Q^2)$ and $\sigma^S(\omega, Q^2)$ for the virtual processes $\gamma_T^* A \to e^+e^- A$ and $\gamma_S^* A \to e^+e^- A$ (where γ_T^* and γ_S^* denote the transverse and scalar/longitudinal photons with helicity $\lambda_T = \pm 1$ and $\lambda_S = 0$, respectively):

$$d\sigma = \sigma^T(\omega, Q^2)\, dn_T(\omega, Q^2) + \sigma^S(\omega, Q^2)\, dn_S(\omega, Q^2). \tag{2.103}$$

Here the coefficients dn_T and dn_S are called the number of transverse and scalar virtual photons (generated by the muon) with energy ω and virtuality Q^2, respectively. The cross sections σ^T and σ^S have been calculated recently in [16]*:

$$\begin{aligned} d\sigma^T = d\sigma_1^T + d\sigma_2^T = \frac{4}{3}\frac{Z^2\alpha^3}{m_e^2}\,[L - f(\nu)] \times \\ \times \left[\frac{m_e^4}{(m_e^2 + Q^2 x_+ x_-)^2} + \frac{2(x_+^2 + x_-^2)m_e^2}{m_e^2 + Q^2 x_+ x_-}\right] dx_+, \end{aligned} \tag{2.104}$$

$$d\sigma^S = d\sigma_1^S + d\sigma_2^S = \frac{4}{3}\frac{Z^2\alpha^3}{m_e^2}\,[L - f(\nu)]\, \frac{4m_e^2 Q^2 x_+^2 x_-^2}{(m_e^2 + Q^2 x_+ x_-)^2}\, dx_+$$

with

$$L = \ln\frac{2\omega x_+ x_-}{m_e} - \frac{1}{2}\ln\frac{m_e^2 + Q^2 x_+ x_-}{m_e^2} - \frac{1}{2}, \tag{2.105}$$

and the function $f(\nu)$ is defined in (2.35). The cross sections $d\sigma_1^{T,S} \propto L$ correspond to the Born contributions and $d\sigma_2^{T,S} \propto -f(\nu)$ to CC. The accuracy of the cross sections (2.104) is determined omitting only terms of the order of

$$\frac{m_e}{\omega}, \quad \frac{Q}{\omega}. \tag{2.106}$$

*In Eqs. (46), (49) and (59) of [16] a factor x_+x_- is missing in the integrands of quantities σ_1^S and σ_2^S.

The number of photons can be found in Sec. 6 and App. D of review [7] (with accuracy $\mathcal{O}(m_\mu^2/E_\mu^2)$, $\mathcal{O}(Q^2/\omega^2)$). They are

$$\begin{aligned} dn_T &= \frac{\alpha}{\pi}(1-y)\left[\left(1-\frac{Q^2_{\min}}{Q^2}\right)D+\lambda C\right]\frac{d\omega}{\omega}\frac{dQ^2}{Q^2},\\ dn_S &= \frac{\alpha}{\pi}(1-y)\left[\left(1+\frac{\lambda}{2}\right)D-\frac{\lambda}{2}C\right]\frac{d\omega}{\omega}\frac{dQ^2}{Q^2}, \end{aligned} \tag{2.107}$$

where

$$\lambda=\frac{1}{2}\frac{y^2}{1-y},\quad Q^2_{\min}=\frac{y^2}{1-y}m_\mu^2,\quad y=\frac{\omega}{E_\mu}. \tag{2.108}$$

For the considered case of muon projectile $C=D=1$, other particles are discussed below. Equations (2.103)–(2.108) are the basis for our following calculations.

Integrating Eq. (2.103) over Q^2 from $Q^2_{\min}$ to infinity (the upper limit can be set to infinity due to the fast convergence of the integral), we obtain the known Born contribution and the new expression for CC:

$$d\sigma_{\mathrm{Coul}}=-\sigma_0 f(\nu)F(x,y)\frac{d\omega}{\omega}\,dx_+ \tag{2.109}$$

with

$$\begin{aligned} F(x,y) &= (1-y)\left\{[(1+\lambda+\xi)a-1-\lambda]\ln\left(1+\frac{1}{\xi}\right)-a+\frac{4-a-\lambda}{1+\xi}\right\},\\ a &= 2(1+x_+^2+x_-^2),\quad \xi=\frac{m_\mu^2}{m_e^2}\frac{y^2}{1-y}x_+x_-. \end{aligned} \tag{2.110}$$

The integration variables can be transformed as follows:

$$\frac{d\omega}{\omega}dx_+=\frac{d\varepsilon_+d\varepsilon_-}{\omega^2}. \tag{2.111}$$

Equation (2.109) describes the energy distribution of e^+ and e^- in CC. In the limit $\xi\ll 1$ (or $y\ll m_e/m_\mu$), the function $F(x,y)$ is approximated by

$$F(x,y)=(1+2x_+^2+2x_-^2)\ln\frac{1}{\xi}-4(x_+^2+x_-^2). \tag{2.112}$$

At $\xi\gg 1$ we obtain

$$F(x,y)=\frac{1}{\xi}[1-y+y^2+2(1-y-y^2)x_+x_-]. \tag{2.113}$$

It is easy to see that the main contribution to $\sigma_{\rm Coul}$ arises from the region

$$m_e^2 \ll \varepsilon_+\varepsilon_- \ll \left(m_e \frac{E_\mu}{m_\mu}\right)^2 . \tag{2.114}$$

Strictly speaking, the cross sections (2.104) are valid for pair-production processes on nuclei. In the collisions of virtual photons with atoms, an atomic screening effect has to be taken into account. For high-energy photons the screening effect changes considerably the differential and total cross section as well as the energy loss for the Born contribution. The reason is that the region of small transverse momenta $k_{1\perp} \lesssim 1/a \sim m_e\alpha Z^{1/3}$ (a denotes the atomic radius) significantly contributes to the cross sections. As a consequence, the function in the Born contribution equivalent to our $F(x,y)$ becomes very complicated and not universal for different atoms (see [25]). On the contrary, the region mainly contributing to CC is determined by the condition $k_{1\perp}, \dots, k_{n\perp} \sim m_e \ll 1/a$. Therefore, the atomic screening effect is negligible in CC and the function $F(x,y)$, as well as some other distributions, is universal and does not depend on atomic properties.

However, if one is interested in very-high-energy pairs effects of the nucleus form factor have to be taken into account both in the Born contributions and in the Coulomb corrections. This happens in the case that the characteristic squared momentum transferred to the nucleus $\sim m_e^2 + Q^2_{\rm min}x_+x_-$ becomes comparable with $(1/R_A)^2$, where R_A is the radius of the nucleus. From this condition it follows that the just mentioned universal behavior is spoilt for $y > 0.5$, where this pair production is strongly suppressed.

2.3.2. Muon Energy Loss. The Coulomb correction to the spectrum of the muon energy loss can be obtained from Eq. (2.109) after integrating over x_+:

$$\begin{gathered} d\sigma_{\rm Coul} = -\sigma_0 f(\nu) F(y) \frac{dy}{y}, \\ F(y) = (1-y)F_1(z) + y^2 F_2(z), \quad z = \frac{m_\mu^2}{m_e^2}\frac{y^2}{1-y}, \end{gathered} \tag{2.115}$$

where

$$\begin{aligned} F_1(z) = {} & \frac{44}{15z} - \frac{16}{15} - \left(\frac{7}{3} + \frac{8z}{15}\right)\ln z + \\ & + \left(-\frac{44}{15z} + \frac{4}{4+z} + \frac{38}{15} + \frac{16z}{15}\right)\sqrt{1+\frac{4}{z}}\,\ln\left(\sqrt{1+\frac{z}{4}} + \sqrt{\frac{z}{4}}\right), \\ F_2(z) = {} & -\frac{4}{3z} - \frac{7}{6}\ln z + \\ & + \left(-\frac{2}{3z} + \frac{8}{z(4+z)} + \frac{7}{3}\right)\sqrt{1+\frac{4}{z}}\,\ln\left(\sqrt{1+\frac{z}{4}} + \sqrt{\frac{z}{4}}\right). \end{aligned} \tag{2.116}$$

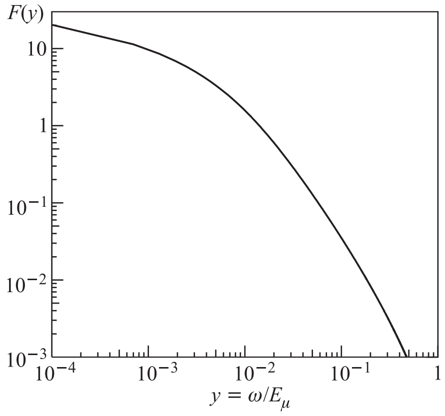

Fig. 9. The function $F(y)$ defined in Eq. (2.115) vs. the fractional energy loss of the muon

The function $F(y)$ is presented in Fig. 9. At small $z \ll 1$ (where $y \ll m_e/m_\mu$), the spectrum has a logarithmic enhancement:

$$F(y) = \left(\frac{7}{3} + \frac{8z}{15}\right) \ln \frac{1}{z} + \frac{20}{9} + \frac{511z}{450} + \ldots, \tag{2.117}$$

whereas at large $z \gg 1$ it is power-like suppressed:

$$F(y) = \frac{1}{z} \left\{ (1-y) \left[\left(2 - \frac{22}{3z}\right) \ln z + 6 + \frac{5}{9z} \right] + \right. \\ \left. + y^2 \left[\left(2 + \frac{1}{z}\right) \ln z + 1 + \frac{1}{2z} \right] \right\} + \mathcal{O}\left(\frac{1}{z^2}\right). \tag{2.118}$$

The approximate expressions (2.117), (2.118) agree with the exact spectrum (2.115) within 1% accuracy everywhere except in the region $y = 0.004{-}0.02$.

From the experimental point of view, of special interest is the relative mean rate of muon energy loss due to pair production (or stopping power) on unit length in matter. This quantity can be calculated as

$$-\frac{1}{E}\frac{dE}{dx} = n \int\limits_{2m_e/E_\mu}^{1} y \frac{d\sigma}{dy}\, dy = n\sigma_0(S_B + S_{\mathrm{Coul}}), \tag{2.119}$$

where n is the number of atoms per unit volume. Formulae and tables for the Born contribution S_B are given in [24]. In particular, for the case without screening

$$S_B = S_0 \left[(1-\delta_1) \ln \frac{E_\mu}{4m_\mu} - 1.771 \right], \tag{2.120}$$

and for complete screening

$$S_B = S_0 \left[(1-\delta_1) \ln \frac{189}{Z^{1/3}} + 0.604 \right], \tag{2.121}$$

where

$$S_0 = \frac{19\pi^2}{12} \frac{m_e}{m_\mu}, \quad \delta_1 = \frac{48}{19\pi^2} \frac{m_e}{m_\mu} \left(\ln \frac{m_\mu}{m_e} \right)^2 = 0.0352. \tag{2.122}$$

From Eqs. (2.115) and (2.119) we derive the Coulomb correction

$$S_{\text{Coul}} = -f(\nu) \int_0^1 F(y)\, dy = -(1-\delta_1)\, f(\nu) S_0. \tag{2.123}$$

When performing the integration, we have used as lower limit zero, since the contribution from region near the threshold $y_{\min} = 2m_e/E_\mu$ can be safely neglected.

2.3.3. Numerical Estimation. To demonstrate the relative importance of CC, we discuss two simple examples: Firstly, we present in Fig. 10 the ratio of the spectral distribution $d\sigma_{\text{Coul}}/dy$ to the corresponding Born cross section

$$\frac{d\sigma_{\text{Coul}}/dy}{d\sigma_B/dy} = -\frac{f(\nu)F(y)}{12F_a(y, E_\mu)}, \tag{2.124}$$

where the universal function $F(y)$ is given in Eq. (2.115) and values for $F_a(y, E_\mu)$ are taken from Table I of [24] for collisions of muons with energy $E_\mu = 86.4$ GeV

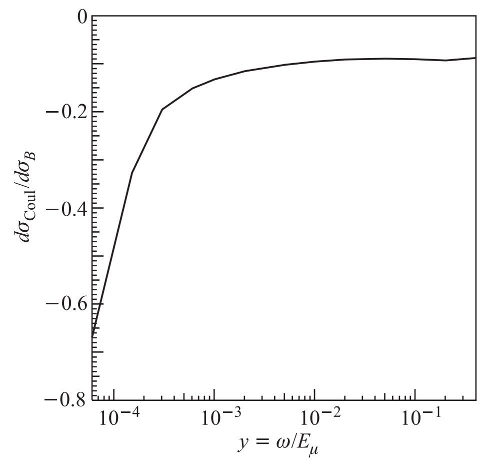

Fig. 10. Ratio of Coulomb to Born energy distribution vs. energy fraction y for muon collisions on Pb target at $E_\mu = 86.4$ GeV

on lead target, $f(\nu) = 0.331$. The presented ratio varies from about -65% to roughly -10% in the considered interval of pair energies.

Secondly, we compare the stopping power $S_{\rm Coul}$ with the Born term in the two limiting cases of Eqs. (2.120) and (2.121). For muon scattering on a Pb target $S_{\rm Coul}/S_B = -15\%$ at $E_\mu = 25$ GeV without screening and –7.7% for the case of complete screening.

It might be useful to present a simple expression for the contribution to $\sigma_{\rm Coul}$ above some cut $\omega > \omega_{\rm cut}$ where this cut is restricted to the region $2m_e \ll \omega_{\rm cut} \ll m_e E_\mu/m_\mu$. From Eq. (2.115) we obtain

$$\sigma_{\rm Coul}(\omega_{\rm cut}) = -\frac{7}{3}\sigma_0\, f(\nu)\left(l^2 + \frac{20}{21}l + \frac{101}{63}\right), \quad l = \ln\frac{m_e E_\mu}{m_\mu \omega_{\rm cut}}. \qquad (2.125)$$

The expression (2.115) does not remain valid close to the threshold $\omega_{\rm min} = 2m_e$. Therefore, from Eq. (2.125) the Coulomb correction to the total pair-production cross section can be obtained only in leading logarithmic approximation by choosing $\omega_{\rm cut} = 2m_e$:

$$\sigma_{\rm Coul} = -\frac{28}{9\pi}\frac{Z^2\alpha^4}{m_e^2} f(\nu)\left(\ln\frac{E_\mu}{2m_\mu}\right)^2. \qquad (2.126)$$

Finally, let us discuss the case that the muon projectile is replaced by other charged projectiles such as electron, pion or proton. For an electron projectile the distributions (2.109) and (2.115) remain valid, changing $m_\mu \to m_e$. However, in these distributions, as well as in the Born contributions, one has to take into account the effect of the identity of the final-state electrons and the bremsstrahlung mechanism of the e^+e^--pair production (according to [29], this changes the result only slightly).

For pion and proton projectiles, in the basic formulae the number of photons should be changed (besides the trivial mass replacements). The numbers of photons are given by Eqs. (2.107) with $C = 0$, $D = F_\pi^2(Q^2)$ for pion and $C = G_M^2(Q^2)$, $D = [4m_p^2 G_E^2(Q^2) + Q^2 G_M^2(Q^2)]/(4m_p^2 + Q^2)$ for proton. Here F_π, G_E and G_M are the pion, proton electric and proton magnetic form factors, respectively, m_p is the proton mass. For the pion case, these changes are essential only for y close to 1 where we should take into account the nucleus form factor, too. For the proton case, the nucleus form factor becomes important for somewhat smaller y where the influence of the proton form factors is still small.

2.4. Multiple Lepton-Pair Production in Relativistic Ion Collisions. The multiplicity and the distribution of lepton pairs produced in the Coulomb fields [14] of two colliding relativistic heavy ions are closely connected to the problem of unitarity. When heavy ions collide at relativistic velocities, their Lorentz contracted electromagnetic fields are sufficiently intense to produce a large number of such pairs. Usually, the process of lepton pair production is considered as pair creation in the classic Coulomb potential of a charge moving along a straight line. Such an approach allows one [35] to investigate the impact-parameter-dependent total probability of the pair creation $P(b)$, which by definition is connected with the total cross section $\sigma = \int P(b)d^2b$. As was noticed in [23], the probability of single-pair production calculated to lowest order in the fine structure constant at small impact parameters exceeds one, thus violating unitarity. This excess begins at impact parameters smaller than the Compton wavelength of the electron $\lambda_c = 1/m = 386$ fm and at energies of practical interest (RHIC & LHC).

Allowance for the finite size of colliding nuclei does not remedy the situation, because that would affect only the impact parameters comparable to the nuclei radii, which are much smaller than the Compton wavelength of the electron $R \ll \lambda_c$.

As was shown in [36], this problem can be solved by taking into account the possibility of multiple pair production, whose relative contribution grows with energy and dominates at small impact parameters. Since this early publication, much work has been done in this area (see, e.g., [37] and references therein) with the statement common for all papers: the probability to produce n lepton pairs in the Coulomb field of heavy ions colliding at fixed impact parameter b can be approximately represented as a Poisson distribution, i.e., $P(b,n) = (W^n(b)/n!)\,\mathrm{e}^{-W(b)}$, where $W(b)$ is the average multiplicity of pairs at a fixed impact parameter.

Because of the somewhat controversial situation in the subject and its importance for the operation of relativistic heavy-ion colliders (RHIC & LHC), in the present subsection we revisit the multiple pair production based on the powerful Sudakov technique, which is very useful in calculations for high-energy processes. Recently, it has been applied [38] to the calculation of Coulomb corrections to single-lepton-pair production in relativistic heavy-ion collisions. Here we extend this approach to get the probability of multiple pair ($n \geqslant 2$) production in relativistic heavy-ion collisions. For heavy ions with the charge numbers satisfying the conditions $Z_1\alpha \sim Z_2\alpha \ll 1$, $Z_1Z_2\alpha \geqslant 1$, one needs full allowance of multiple Coulomb interaction of colliding nuclei, whereas the secondary interaction of produced pairs (real or virtual) with the Coulomb fields of colliding ions can be neglected.

2.4.1. The Amplitude of n-Pair Production Process. The typical FD describing the n-lepton-pair production in the collision of relativistic nuclei with atomic numbers A_1, A_2, with n_e exchanged photons between colliding nuclei as well as screening effects, e.g., the insertions of n_s LBL scattering blocks, is drawn in Fig. 11.

Upper and lower blocks in Fig. 11 describe amplitudes of interaction of virtual photons with nuclei. They contain the complete set of $(n_e + n + 2n_s)!$ Feynman diagrams. To avoid the multiple counting in what follows, we will multiply the relevant amplitude by the factor $1/(n_e!n_s!(2!)^{2n_s})$.

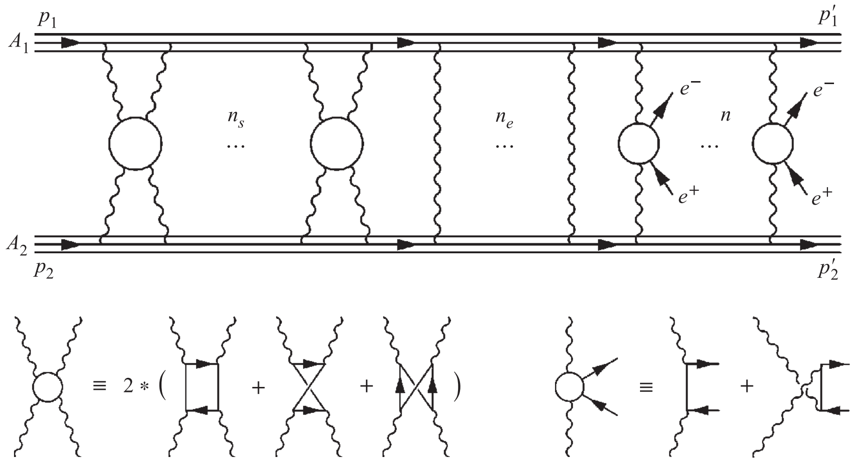

Fig. 11. The peripheral process of creation of n lepton pairs with n_e photon exchanges between nuclei A_1, A_2 and n_s light-by-light scattering blocks

As was mentioned above, we restrict ourselves to ions with charge numbers such that

$$Z_1\alpha \sim Z_2\alpha \ll 1, \quad Z_1 Z_2\alpha \geqslant 1, \tag{2.127}$$

which permits us to omit the multiphoton exchanges between the produced pairs and colliding ions. The dominant mechanism is a production of a single lepton pair per collision of equivalent photons, i.e., one lepton pair per two-photon ladder. The alternative mechanism of multiple pair production per collision of two equivalent photons is suppressed by inverse powers of Z_1Z_2.

For the description of a peripheral process of n-lepton-pair creation, i.e., the process

$$\begin{aligned} A_1(Z_1,p_1) + A_2(Z_2,p_2) \to A_1(Z_1,p_1') + A_2(Z_2,p_2') +& \\ + e_+e_-(r_1) + \ldots + e_+e_-(r_n), \quad r_i = q_+^i + q_-^i, \end{aligned} \tag{2.128}$$

it is convenient to use the Sudakov parameterization for the four-momentum of all exchanged photons (for details, see [38])

$$\begin{gathered} k_i = \alpha_i\tilde{p}_2 + \beta_i\tilde{p}_1 + k_{i\perp}, \quad d^4k_i = \frac{s}{2}d\alpha_i d\beta_i d^2k_{i\perp}, \\ s = (p_1+p_2)^2, \quad s \gg p_i^2 = M_i^2 \gg m^2, \\ \tilde{p}_1 = p_1 - p_2\frac{p_1^2}{s}, \quad \tilde{p}_2 = p_2 - p_1\frac{p_2^2}{s}, \\ \tilde{p}_1^2 = \tilde{p}_2^2 = \mathcal{O}\left(\frac{M^6}{s^2}\right), \quad \tilde{p}_1k_{i\perp} = \tilde{p}_2k_{i\perp} = 0, \quad s = 2p_1p_2 = 2\tilde{p}_1\tilde{p}_2. \end{gathered} \tag{2.129}$$

Here $\tilde{p}_i$ are light-like four-vectors built from p_i, M_i are the masses of colliding nuclei, m and s are the electron mass and the total center-of-mass energy.

The denominators of intermediate states of the nucleon Green functions for upper and lower blocks are the same and have the following form:

$$-s\sum_i \alpha_i - \Big(\sum_i \mathbf{k}_i\Big)^2 + i0, \quad s\sum_i \beta_i - \Big(\sum_i \mathbf{k}_i\Big)^2 + i0. \tag{2.130}$$

Peripheral process is characterized by small values of longitudinal Sudakov parameters α_i, β_i and the transverse momenta of the order of electron mass

$$|\alpha_i| \sim |\beta_i| \ll 1, \quad -k_{i\perp}^2 \sim m^2. \tag{2.131}$$

Further simplification follows from the form of the nominators of the exchanged photon Green functions (we work in the Feynman gauge). Using the Gribov representation for the metric tensor

$$g_{\mu\nu} = g_{\mu\nu}^{\perp} + \frac{2}{s}\Big(\tilde{p_1}^{\mu}\tilde{p_2}^{\nu} + \tilde{p_1}^{\nu}\tilde{p_2}^{\mu}\Big), \tag{2.132}$$

it is easy to show that for the typical conversion of the nuclei currents $J_\mu(p_1)$ and $J^\mu(p_2)$ only one term, which contains the scalar products of a nucleus current with a four-momentum of another nucleus, becomes relevant (with power accuracy):

$$J_\mu(p_1)J^\mu(p_2) \approx \frac{2}{s}J_\lambda(p_1)p_2^\lambda J_\sigma(p_2)p_1^\sigma\left(1+\mathcal{O}\Big(\frac{M^2}{s}\Big)\right). \tag{2.133}$$

It can be seen that the quantity $J_\mu(p_1)p_2^\mu/s$ remains finite with the large values of s. This fact provides great simplification of the spinor structure of the amplitude

$$\begin{aligned}\bar{u}(p_1')\tilde{p}_2(p_1+\chi_1+M_1)\tilde{p}_2\cdots(p_1+\chi_N+M_1)\tilde{p}_2u(p_1) &\approx s^{N+1}N_1,\\ \bar{u}(p_2')\tilde{p}_1(p_2+\eta_1+M_2)\tilde{p}_1\cdots(p_2+\eta_N+M_2)\tilde{p}_1u(p_2) &\approx s^{N+1}N_2,\end{aligned} \tag{2.134}$$

$$N_1 = \frac{1}{s}\bar{u}(p_1')\hat{p}_2u(p_1), \quad N_2 = \frac{1}{s}\bar{u}(p_2')\hat{p}_1u(p_2).$$

Besides, we have $\sum|N_1|^2 = \sum|N_2|^2 = 2$ for the nuclei with the spin 1/2 and $|N_1|^2 = |N_2|^2 = 1$ for the scalar one. Using the identity

$$\sum_{\text{perm}}\frac{1}{\alpha_{i_1}}\frac{1}{\alpha_{i_1}+\alpha_{i_2}}\cdots\frac{1}{\sum\limits_{j=1}^{N}\alpha_{i_j}} = \prod_{i=1}^{N}\frac{1}{\alpha_i}, \tag{2.135}$$

one can be convinced that the amplitude describing the upper and lower blocks in Fig. 11 can be put in the form

$$I_1 = N_1 \prod_{i=1}^{N} \left(\frac{s}{-s\alpha_i + i0} + \frac{s}{s\alpha_i + i0} \right),$$
$$I_2 = N_2 \prod_{i=1}^{N} \left(\frac{s}{-s\beta_i + i0} + \frac{s}{s\beta_i + i0} \right) \qquad (2.136)$$

with $N = n_e + 2n_s + n - 1$.

These expressions contain all dependences on Sudakov parameters α_i, β_i (the 4-momenta of exchanged photons in the peripheral kinematics in denominators of their Green functions can be considered as Euclidean two-vectors $k_i^2 = s\alpha_i\beta_i + k_{i\perp}^2 \approx k_{i\perp}^2 = -\mathbf{k}_i^2$).

At this stage the integration over Sudakov parameters can be done, because the dependence of the amplitude on α_i, β_i provides the convergence of the relevant integrals

$$\int I_1 \prod_{i=1}^{N} d\alpha_i = (2\pi i)^N N_1, \quad \int I_2 \prod_{i=1}^{N} d\beta_i = (2\pi i)^N N_2. \qquad (2.137)$$

Let us now consider the single-pair production. The amplitude of the process (2.128) in its lowest order (Born approximation) reads [38]

$$M_{(0)}^{(1)} = is(8\pi\alpha)^2 Z_1 Z_2 N_1 N_2 \frac{B_{\alpha\beta} p_1^\alpha p_2^\beta}{s\mathbf{q}_1\mathbf{q}_2}, \quad B_{\alpha\beta} = \bar{v}(q_+) O_{\alpha\beta} u(q_-), \qquad (2.138)$$

$B_{\alpha\beta}$ is the Compton tensor [38] for pair creation by two virtual photons with polarization vectors $e_1(q_1)$, $e_2(q_2)$; $q_{1(2)}$ are the 4-momenta of exchanged photons and $r = q_+ + q_-$. Strictly speaking, the squares of these 4-vectors q_i^2 do not vanish in the limit $\mathbf{q}_i \to 0$. This fact becomes essential when one calculates the total cross section of a single-pair production process. For the case of two or more pair production (which is our case), the replacement $q_i^2 = -\mathbf{q}_i^2$ can safely be done.

Using the gauge invariance

$$q_1^\alpha B_{\alpha\beta} = q_2^\beta B_{\alpha\beta} = 0, \qquad (2.139)$$

one can perform the replacement

$$\frac{B_{\alpha\beta} p_1^\alpha p_2^\beta}{s} = \frac{B_{\alpha\beta} e_1^\alpha e_2^\beta}{\tilde{s}_1} |\mathbf{q}_1||\mathbf{q}_2|, \quad e_i^\alpha = \frac{q_{i\perp}^\alpha}{|\mathbf{q}_i|}, \quad \tilde{s}_1 = s\alpha_2\beta_1. \qquad (2.140)$$

The quantity $\tilde{s}_1$ is related to the square of the invariant mass of a pair:

$$s_1 = (q_1 + q_2)^2 = \tilde{s}_1 - (\mathbf{q}_1 + \mathbf{q}_2)^2 = (q_+ + q_-)^2. \tag{2.141}$$

Two-dimensional vectors e_i can be interpreted as polarization vectors of exchanged virtual photons.

Using (2.139)–(2.141), one can rewrite the Born amplitude (2.138) in a form

$$M_{(0)}^{(1)} = isN_1N_2B(q_1, q_2), \tag{2.142a}$$

$$B(q_1, q_2) = (8\pi\alpha)^2 Z_1 Z_2 \frac{B_{\alpha\beta}e_1^\alpha e_2^\beta}{\tilde{s}_1|\mathbf{q}_1||\mathbf{q}_2|}. \tag{2.142b}$$

Now we are able to construct the amplitude for the process of n-pair production. Bearing in mind the expressions (2.137), the matrix element of two-pair production can be represented as the convolution of two Born terms from the expression (2.142b):

$$M_{(0)}^{(2)} = i^2 sN_1N_2 \int B(k, k - r_1)B(q - k, q - r_2 - k)\frac{d^2\mathbf{k}}{8\pi^2}. \tag{2.143}$$

A straightforward generalization to the matrix element in the case of n-pair production reads

$$M_{(0)}^{(n)} = i^n sN_1N_2 \int \prod_{i=1}^{n-1} \left(B(k_i, k_i - r_i)\frac{d^2k_i}{8\pi^2} \right) B(h, h - r_n), \tag{2.144}$$

$$h = q - \sum_{i=1}^{n-1} k_i. \tag{2.145}$$

Thus, one can see that the amplitude for multiple pair production is solely determined by the convolution of the amplitudes corresponding to single-pair production.

In the language of the AGK unitarity rules, this result can be interpreted as unitarity cut through all exchanged Pomerons [38].

2.4.2. The Coulomb Exchanges between Ions. Let us now consider the effect of m photon exchanges between nuclei A_1, A_2. The arguments given above lead to the following matrix element for the process of n-pair production with m photon exchanges among the colliding ions:

$$M_{(m)}^{(n)} = \frac{i^n sN_1N_2}{m!} \int \prod_{j=1}^{m} \left(\frac{-i\alpha Z_1 Z_2}{\boldsymbol{\chi}_j^2 + \lambda^2} \frac{d^2\boldsymbol{\chi}_j}{\pi} \right) \times$$
$$\times \int \prod_{i=1}^{n-1} \left(B(k_i, k_i - r_i)\frac{d^2\mathbf{k}_i}{8\pi^2} \right) B(k_n, k_n - r_n),\ k_n = q - \sum_{i=1}^{n-1} k_i - \sum_{i=1}^{m} \chi_i. \tag{2.146}$$

Another effect which we take into account is the possibility of the ion–ion interaction through the LBL blocks (screening effect in Fig. 12), which in the AGK language [39] is equivalent to the exchange by additional uncut Pomerons. It is associated with the iteration of a typical kernel

$$L \int Y(\mathbf{l})\, d^2\mathbf{l}, \tag{2.147a}$$

$$Y(\mathbf{l}) = \frac{(\alpha^2 Z_1 Z_2)^2}{32\pi^4} \int \frac{P}{|\mathbf{l}_1||\mathbf{l}_2||\mathbf{l}_1-\mathbf{l}||\mathbf{l}_2+\mathbf{l}|} d^2\mathbf{l}_1 d^2\mathbf{l}_2 \frac{d\tilde{s}_1}{\tilde{s_1}^2}, \tag{2.147b}$$

$$P = \Pi^{\alpha\beta\gamma\delta} e_1^\alpha(l_1) e_2^\beta(l_1-l) e_3^\gamma(l_2) e_4^\delta(l_2+l), \tag{2.147c}$$

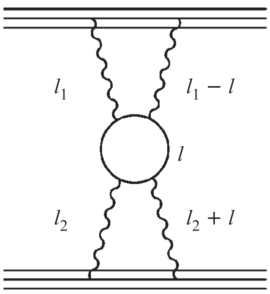

Fig. 12. Typical kernel of the ion–ion interaction through the LBL blocks

where we rearrange the «extra» phase volume of longitudinal Sudakov parameters α_2, β_1 in terms of invariant mass square of LBL block and extract explicitly the boost degree of freedom of LBL block:

$$\int \frac{d\alpha_2 d\beta_1}{s(\alpha_2\beta_1)^2} = \int \frac{d\beta_1}{\beta_1} \int \frac{d\tilde{s}_1}{\tilde{s}_1^2} = L \int \frac{d\tilde{s}_1}{\tilde{s}_1^2}, \tag{2.148}$$

$$L = \ln(\gamma_1\gamma_2), \quad \tilde{s}_1 = (l_1+l_2)^2 > 4m^2.$$

The structure (2.147a) entered the matrix element (2.146) in the compact form

$$\frac{1}{n_s!} \prod_{i=1}^{n_s} \Big(LY(\mathbf{l}_i) d^2\mathbf{l}_i \Big). \tag{2.149}$$

The real part of (2.147c) (equal to one half of its s-channel discontinuity) is related with (2.142b) as

$$\mathrm{Re}\, \Pi^{\alpha\beta\gamma\delta} e_1^\alpha(l_1) e_2^\beta(l_1-l) e_3^\gamma(l_2) e_4^\delta(l_2+l) = \frac{1}{2} \int B_{\alpha\beta}(l_1, r-l_1) e_1^\alpha(l_1) e_2^\beta(r-l_1) \times$$
$$\times B_{\gamma\delta}(l_1-l, r+l-l_1) e_1^\gamma(l_1-l) e_2^\delta(r+l-l_1)\, d\Phi_r, \tag{2.150}$$

where $d\Phi_r$ is the phase volume of the intermediate pair:

$$d\Phi_r = \frac{\delta^4(r-q_+-q_-) d^3q_+\, d^3q_-}{(2\pi)^2 2\varepsilon_+ 2\varepsilon_-}. \tag{2.151}$$

We will show later that the imaginary part of Π is irrelevant either for the total cross section or for the probability of n-pair production distribution.

2.4.3. The Impact-Parameter Representation for the Amplitude. The last step in building the matrix element for the process of n-real-pair creation consists in transformation of the above-obtained expressions in the impact-parameter representation and summation over all eikonal photons and LBL blocks. For this aim, we introduce the unity factor through the identity:

$$\int \delta^2\left(\mathbf{k}_n - \mathbf{q} + \sum_{i=1}^{n-1}\mathbf{k}_i + \sum_{i=1}^{n_s}\boldsymbol{\chi}_i + \sum_{i=1}^{n}\mathbf{l}_m\right) d^2\mathbf{k}_n = \frac{1}{4}\int \mathrm{e}^{-i\mathbf{q}\boldsymbol{\rho}}\times$$
$$\times \exp\left[i\boldsymbol{\rho}\left(\mathbf{k}_n + \sum_{i=1}^{n-1}\mathbf{k}_i + \sum_{i=1}^{n_s}\boldsymbol{\chi}_i + \sum_{i=1}^{n}\mathbf{l}_m\right)\right]\frac{d^2\mathbf{k}_n}{\pi}\frac{d^2\boldsymbol{\rho}}{\pi} = 1. \quad (2.152)$$

Using this expression, the summation in n_e and n_s can be easily done with the result

$$M^{(n)} = \frac{i^n\pi s}{2}N_1N_2\int \mathrm{e}^{-i\mathbf{q}\boldsymbol{\rho}}\,\mathrm{e}^{i\Psi(\rho\lambda)}\,\mathrm{e}^{-L[A(\rho)/2+i\varphi(\rho)]}\times$$
$$\times\prod_{i=1}^{n}\tilde{B}(\boldsymbol{\rho},\mathbf{r}_i)\frac{d^2\boldsymbol{\rho}}{\pi}, \quad n\geqslant 2, \quad (2.153)$$

with

$$\frac{A(\rho)}{2} + i\varphi(\rho) = \int Y(\mathbf{l})\,\mathrm{e}^{i\mathbf{l}\boldsymbol{\rho}}\frac{d^2\mathbf{l}}{\pi},$$
$$\tilde{B}(\boldsymbol{\rho},\mathbf{r}_i) = \int B(\mathbf{k},\mathbf{k}-\mathbf{r}_i)\,\mathrm{e}^{i\mathbf{k}\boldsymbol{\rho}}\frac{d^2\mathbf{k}}{8\pi^2}, \quad (2.154)$$

$$\Psi(\rho\lambda) = -\alpha Z_1Z_2\int\frac{\mathrm{e}^{i\boldsymbol{\chi}\boldsymbol{\rho}}}{\boldsymbol{\chi}^2+\lambda^2}\frac{d^2\boldsymbol{\chi}}{\pi} = -2\alpha Z_1Z_2K_0(\lambda\rho), \quad (2.155)$$

where $K_0(\lambda\rho)$ is modified Bessel function (Macdonald function).

The phase volume of final state which consists of the scattered nuclei and n pairs can be written in the following form:

$$d\Gamma_{n+2} = \prod_{i=1}^{n}\left(\frac{d^3q_+\,d^3q_-}{(2\pi)^6 2\varepsilon_+ 2\varepsilon_-}\right)\frac{1}{(2\pi)^2}\frac{d^3p_1'\,d^3p_2'}{2\varepsilon_1' 2\varepsilon_2'}\delta^4\left(p_1+p_2-p_1'-p_2'-\sum_{i=1}^{n}r_i\right) =$$
$$= \prod_{i=1}^{n}\left(\frac{L}{(2\pi)^4}\frac{d^2\mathbf{r}_i}{2}ds_i\,d\Phi_i\right)\frac{d^2\mathbf{q}}{2s(2\pi)^2}, \quad (2.156)$$

with $q = p'_{1\perp}$.

The cross section of n-pair production has the form

$$d\sigma_n = \frac{1}{8s}\frac{|M_n|^2}{n!}d\Gamma_{n+2}. \tag{2.157}$$

Statistical factor $1/n!$ is included to take into account the identity of pairs. Using the expressions (2.152)–(2.156), we get

$$\frac{d\sigma_n}{d^2\rho} = P_n(\rho), \quad P_n(\rho) = \frac{(LA_1(\rho))^n}{n!}\,\mathrm{e}^{-LA_1(\rho)}, \quad n \geqslant 2 \tag{2.158}$$

with

$$A_1(\rho) = \frac{1}{2^5\pi^4}\int |\tilde{B}(\rho, r)|^2 ds_1\, d^2\mathbf{r}\, d\Phi_r. \tag{2.159}$$

It can be easily recognized that for $A(\rho)$ from (2.154)

$$A(\rho) = A_1(\rho), \tag{2.160}$$

thus confirming the Poisson character of probability distribution in impact-parameter representation.

Let us mention that the effect of eikonal photons, as well as the imaginary part of the amplitude corresponding to LBL blocks, does not modify the total cross section as well as differential cross section integrated over phase volume of final nuclei. Really, integrating the square of the amplitude (2.153) over the phase volume, one immediately obtains

$$\int \mathrm{e}^{i\mathbf{q}(\boldsymbol{\rho}_1-\boldsymbol{\rho}_2)}\,\mathrm{e}^{i\{[\psi(\rho_1)-\psi(\rho_2)]-L[\varphi(\rho_1)-\varphi(\rho_2)]\}} f(\rho_1) f(\rho_2)\frac{d^2\mathbf{q}}{\pi}\frac{d^2\boldsymbol{\rho}_1}{\pi}\frac{d^2\boldsymbol{\rho}_2}{\pi} = \\ = \int f^2(\rho)\frac{d^2\boldsymbol{\rho}}{\pi}.$$

Nevertheless, the exclusive cross section is sensitive to both these factors.

The expression (2.159) can be simplified if one neglects the dependence of Compton tensor on external photons virtualities

$$B_{\alpha\beta}(k, r)\, e^\alpha\, e^\beta \to B_{\alpha\beta}(0, r)\, e^\alpha\, e^\beta \tag{2.161}$$

and use the well-known relation [4]:

$$\int\limits_{4m^2}^{\infty} \sum \left|B_{\alpha\beta}(0, r)\, e^\alpha\, e^\beta\right|^2 \frac{ds_1\, d\Phi_r}{s_1^2} = \\ = \frac{1}{8\pi^2\alpha^2}\int\limits_{4m^2}^{\infty}\frac{ds_1}{s_1}\sigma_{\gamma\gamma\to e^+e^-}(s) = \frac{7}{36\pi m^2}. \tag{2.162}$$

As a result, the expression (2.159) can be cast in the form

$$A(\rho) = \frac{7}{18\pi^2 m^2}(\alpha^2 Z_1 Z_2)^2 I(\rho),$$

$$I(\rho) = \int^m \frac{\mathrm{e}^{i\boldsymbol{\rho}(\mathbf{k}_1-\mathbf{k}_2)}}{|\mathbf{k}_1||\mathbf{k}_1-\mathbf{r}||\mathbf{k}_2||\mathbf{k}_2-\mathbf{r}|}\frac{d^2\mathbf{r}}{\pi}\frac{d^2\mathbf{k}_1}{\pi}\frac{d^2\mathbf{k}_2}{\pi} = \tag{2.163}$$

$$= \int^m \frac{\mathrm{e}^{i\boldsymbol{\chi}\boldsymbol{\rho}}}{|\mathbf{k}||\mathbf{k}-\boldsymbol{\chi}||\mathbf{k}'||\mathbf{k}'+\boldsymbol{\chi}|}\frac{d^2\boldsymbol{\chi}}{\pi}\frac{d^2\mathbf{k}}{\pi}\frac{d^2\mathbf{k}'}{\pi} = \tag{2.164}$$

$$= \int \mathrm{e}^{i\boldsymbol{\chi}\boldsymbol{\rho}} \ln^2\left(\frac{m^2}{\boldsymbol{\chi}^2}\right)\frac{d^2\boldsymbol{\chi}}{\pi} \approx \frac{16}{\rho^2}\left(\ln(\rho m) + \mathcal{O}(1)\right), \tag{2.165}$$

where we introduce the cut-off parameter $|k| < m$ as a result of the fast decreasing of matrix element of pair production by two photons. For the case of heavy-lepton production (μ or τ), the upper limit must be replaced by quantity Q, which can be associated with maximal momentum transferred to nucleus without its disintegration. For the case $\rho\, m \gg 1$, one has

$$A(\rho) \approx \frac{56}{9}\frac{(\alpha^2 Z_1 Z_2)^2}{\pi^2(\rho m)^2}\left(\ln(\rho m) + O(1)\right), \tag{2.166}$$

which is in agreement with the result obtained in [37].

Our formula (2.158) can be applied to the case $n = 0$ (the probability of elastic nuclei scattering). The case $n = 1$ needs a bit more accurate consideration. The expression for σ_1 can be cast in the following form:

$$\sigma_1 = \sigma_B + L\int A(\rho)\left(\mathrm{e}^{-LA(\rho)} - 1\right) d^2\boldsymbol{\rho}. \tag{2.167}$$

The first term σ_B corresponds to the leading order of the Racah formula (see, for instance, [23]) for the cross section in Born approximation. Inferring (2.167), one has to take into account the longitudinal components of momenta of exchanged photons which create the pair. The second term is responsible for the unitarity corrections to the total cross section.

2.5. Measuring the Deviation from Rutherford Formulae. Modern experiments with heavy ion–lepton collisions provide the possibility to measure the deviation of cross section of small-angle electron (positron)–ion elastic scattering from the Rutherford formula due to taking into account the multiple virtual-photon exchange.

First correct results for calculation of the lowest-order correction for the cross section of elastic scattering of electron on the external Coulomb field of the target nuclei with the charge Z were obtained about 60 years ago [5, 32].

It was found that the correction to the Rutherford cross section $d\sigma_R/dO = (Z\alpha)^2/(4E^2\sin^4(\theta/2))$ has a form

$$\frac{d\sigma^{(2)}}{dO} = \frac{\pi(Z\alpha)^3 E}{4p^3\sin^3(\theta/2)}(1-\sin(\theta/2)), \tag{2.168}$$

and, besides even for the case of unpolarized initial electron the scattered one obtains the polarization

$$\boldsymbol{\xi} = \frac{2Z\alpha pm}{E^2}\frac{\sin^3(\theta/2)\ln\sin(\theta/2)}{(1-v^2\sin^2(\theta/2))\cos(\theta/2)}\boldsymbol{\nu}, \tag{2.169}$$

where $\cos\theta = \mathbf{nn}'$, $\boldsymbol{\nu} = [\mathbf{n},\mathbf{n}']$ and $\mathbf{n}$, $\mathbf{n}'$ are the unit vectors along the directions of the initial and the scattered electrons motion (we imply the rest frame of the heavy ion); θ is the scattering angle; E, p are the energy and the value of the 3-momentum of the electrons. This correction changes the sign for the case of positron scattering by the same nuclei. It is the reason of the nonzero charge asymmetry, which in the lowest order of PT has a form (in relativistic case)

$$A^{(1)} = \frac{d\sigma^{e_-Z} - d\sigma^{e_+Z}}{2d\sigma_R} = \pi(Z\alpha)\sin(\theta/2)(1-\sin(\theta/2)). \tag{2.170}$$

In papers of the seventies [33, 34] the formula which takes into account all orders of expansion on the $x = Z\alpha/v$ (v is the velocity of electron in the rest frame of the nuclei) parameter was obtained for the asymmetry, using the so-called eikonal approximation. The answer is

$$A^{\infty} = A = \pi x\cos(\varphi(x))\sin(\theta/2) + \mathcal{O}(\theta^2), \tag{2.171}$$

with

$$\cos(\varphi(x)) = \mathrm{Re}\,\Omega(x), \quad \Omega(x) = \frac{\Gamma(1/2+ix)\Gamma(1-ix)}{\Gamma(1/2-ix)\Gamma(1+ix)}. \tag{2.172}$$

The expansion of $\varphi(x)$ has a form

$$\varphi(x) = -4\left[(\ln 2)x - \xi_3 x^3 + \ldots + (-1)^n\frac{x^{2n+1}}{2n+1}(2^{2n}-1)\xi_{2n+1} + \ldots\right], \quad n > 1, \tag{2.173}$$

with the Riemann $\xi_n = \sum\limits_1^{\infty}(1/k^n)$ function. At values comparable with unity or exceeding it, we have $\cos(\varphi(x)) \sim 1/(4x)$. In the paper [34] this result was obtained by direct summing of the contribution of Feynman amplitudes with the multiphoton exchange between lepton and the nuclei. It was noted that the real parameter of expansion is $Z\alpha/v$, where $v = p/E$ is the velocity of the lepton. So, for instance, in the limit $x \gg 1$ the asymmetry does not depend on x: $A = (\pi/4)\sin(\theta/2)$.

Following the paper [33] (see also [1]), we obtain for the high-energy elastic scattering amplitude of electron with energy E on Coulomb field in eikonal approximation

$$f(q) = -iE \int_0^\infty \rho \, d\rho \, J_0(\rho q) \, \mathrm{e}^{i\kappa(\rho)}, \tag{2.174}$$

where ρ is the impact parameter; $q = 2E\sin(\theta/2)$ is the momentum transferred to the nuclei; θ is the electron scattering angle (Laboratory r.f. implied); $J_0(z)$ is the Bessel function.

We use the eikonal phase in the first and second approximation on the Coulomb field [1] $\kappa(\rho) = \kappa_0(\rho) + \kappa_1(\rho)$ with

$$\kappa_0(\rho) = -\int_{-a}^{a} V(\rho, z) dz, \quad \kappa_1(\rho) = -\frac{\rho^2}{E}\int_{-\infty}^{\infty} \frac{\partial}{\partial \rho^2} V^2(\rho, z)\, dz,$$

with the potential of Coulomb field

$$V(\rho, z) = \frac{\nu \,\mathrm{sign}\,(e)}{\sqrt{\rho^2 + z^2}}, \quad \nu = Z\alpha, \tag{2.175}$$

and a is the Coulomb regularizing parameter $a \gg \rho$. A simple calculation gives ($\mathrm{sign}\,(e) = 1$)

$$\kappa_0(\rho) = 2\nu \ln\left(\frac{\rho}{2a}\right), \quad \kappa_1(\rho) = \frac{\pi\nu^2}{2E\rho}. \tag{2.176}$$

Keeping in mind $|\kappa_0| \gg |\kappa_1|$, we obtain for the amplitude

$$f(q) = -iE \int_0^\infty \rho \, d\rho \, J_0(\rho q) \left(\frac{\rho}{2a}\right)^{2i\nu} \left(1 + i\frac{\pi\nu^2}{2\rho E}\right). \tag{2.177}$$

Providing the ρ integration, we use [21]

$$\int_0^\infty x^\mu J_0(qx)\, dx = 2^\mu (q)^{-\mu-1} \frac{\Gamma((1+\mu)/2)}{\Gamma((1-\mu)/2)}. \tag{2.178}$$

As a result, we obtain

$$f(q) = -\frac{\nu E}{2q^2}(aq)^{-2i\nu}\frac{\Gamma(1+i\nu)}{\Gamma(1-i\nu)}\left[1-\frac{\pi\nu q}{4E}\Omega(\nu)\right], \tag{2.179}$$

with $\Omega(x)$ given above. For the cross section we obtain

$$d\sigma = d\sigma_R\left[1-\pi x\sin\left(\frac{\theta}{2}\right)\mathrm{Re}\,\Omega(x)\right]. \tag{2.180}$$

Expression for the asymmetry (2.171) follows immediately.

Acknowledgements. We are grateful to many our collaborators who generously permit us to use the results obtained in common papers. One of us (EAK) is grateful to Lev Lipatov, Viktor Fadin and Valery Serbo for many years collaborations and numerous detailed and valuable discussions. We are also grateful to S. Bakmaev for help and encouragement. This work was supported by grants MK-1607.2008.2, INTAS-05-1000008-8328.

We present our apologies to authors working in the same area, whose papers unfortunately escaped our attention.

REFERENCES

1. *Akhiezer A. I., Berestetskii V. B.* Quantum Electrodynamics. M.: Nauka, 1959; 1981.
2. *Berestetskii V. B., Lifshitz E. M., Pitaevskii L. B.* Quantum Electrodynamics. M.: Nauka, 1989.
3. *Vinokurov E. A., Kuraev E. A., Merenkov N. P.* Radiative Corrections to e^+e^- Pair Production Induced by High Energy Photons Incident on Electrons or Nuclei // Zh. Eksp. Teor. Fiz. 1974. V. 66. P. 1916.
4. *Kuraev E. A., Lipatov L. N.* Electron and Muonic Production in e^-e^- and e^+e^- Colliding Beams // Yad. Fiz. 1972. V. 16. P. 1060.
5. *Landau L. D., Lifschitz E. M.* Production of Electrons and Positrons by a Collision of Two Particles // Phys. Z. Sowjetunion. 1934. V. 6. P. 244.
6. *Racah G.* Sulla nastica di coppie per urti di particelle eletrizzate // Nuovo Cim. 1937. V. 14. P. 93.
7. *Budnev V. M. et al.* The Two Photon Particle Production Mechanism. Physical Problems. Applications. Equivalent Photon Approximation // Phys. Rep. 1974. V. 15. P. 181.
8. *Kuraev E. A., Schiller A., Serbo V. G.* The Process $\gamma\gamma \to \pi^+\pi^-e^+e^-$ for High-Energy $\gamma\gamma$ Beams // Nucl. Phys. B. 1985. V. 256. P. 189; 211.
9. *Amsler C. et al.* Particle Data Group // Phys. Lett. B. 2008. V. 667. P. 1.

10. *Hencken K., Kuraev E. A., Serbo V.* Exclusive and Inclusive Muon Pair Production in Collisions of Relativistic Nuclei // Phys. Rev. C. 2007. V. 75. P. 034903; hep-ph/0606069.

11. *Baur G. et al.* Coherent Gamma Gamma and Gamma A Interactions in Very Peripheral Collisions at Relativistic Ion Colliders // Phys. Rep. 2002. V. 364. P. 359; hep-ph/0112211.

12. *Klein S. R.* Localized Beampipe Heating Due to e^- Capture and Nuclear Excitation in Heavy Ion Colliders // Nucl. Instr. Meth. A. 2001. V. 459. P. 51; physics/0005032.

13. *Ivanov D. Y., Schiller A., Serbo V. G.* Large Coulomb Corrections to the e^+e^- Pair Production at Relativistic Heavy Ion Colliders // Phys. Lett. B. 1999. V. 454. P. 155; hep-ph/9809449.

14. *Bartos E. et al.* Multiple Lepton Pair Production in Relativistic Ion Collisions // Phys. Lett. B. 2002. V. 538. P. 45; hep-ph/0204327.

15. *Baur G. et al.* Multiphoton Exchange Processes in Ultraperipheral Relativistic Heavy Ion Collisions // Nucl. Phys. A. 2003. V. 729. P. 787; nucl-th/0307031.

16. *Ivanov D., Melnikov K.* Lepton Pair Production by a High Energy Photon in a Strong Electromagnetic Field // Phys. Rev. D. 1998. V. 57. P. 4025; hep-ph/9709352.

17. *Bethe H. A., Maximon L. C.* Theory of Bremsstrahlung and Pair Production: I. Differential Cross Section // Phys. Rev. 1954. V. 93. P. 768.

18. *Olsen H., Maximon L. C.* Photon and Electron Polarization in High-Ernergy Bremsstrahlung and Pair Production with Screening // Phys. Rev. 1959. V. 114. P. 887.

19. *Maximon L. C., Olsen H.* Measurement of Linear Photon Polarization by Pair Production // Phys. Rev. 1962. V. 126. P. 310.

20. *Haug E.* Bremsstrahlung and Pair Production in the Field of Free Electrons // Z. Naturforsch. A. 1975. V. 30. P. 1099;
Haug E. Simple Analytic Expressions for the Total Cross-Section for Gamma E Pair Production // Z. Naturforsch. A. 1981. V. 36 . P. 413.

21. *Gradshteyn I. S., Ryzhik I. M.* Table of Integrals, Series, and Products. Boston: Acad. Press, 1994.

22. *Moliere G.* Theorie der Streuung schneller geladener Teilchen I Einzelstreuung am abgeschermten Coulomb-Feld // Z. Naturforsch. A. 1947. V. 2. P. 133.

23. *Bertulani C. A., Baur G.* Electromagnetic Processes in Relativistic Heavy Ion Collisions // Phys. Rep. 1988. V. 163. P. 299.

24. *Kelner S. R., Kotov Yu. D.* A Contribution to the Problem of Electron and Muon Pair Production by Cosmic Ray Muons // Yad. Fiz. 1969. V. 9. P. 1210.

25. *Nikishov A. I.* Energy Spectrum of e^+e^- Pair Created in Muon Collision with an Atom // Sov. J. Nucl. Phys. 1978. V. 27. P. 677 (Yad. Fiz. 1978. V. 27. P. 1281).

26. *Van Ginneken A.* Energy Loss and Angular Characteristics of High-Energy Electromagnetic Processes // Nucl. Instr. Meth. A. 1986. V. 251. P. 21.

27. *Davies H., Bethe H. A., Maximon L. C.* Theory of Bremsstrahlung and Pair Production: II. Integral Cross-Section for Pair Production // Phys. Rev. 1954. V. 93. P. 788.

28. *Nikishov A. I., Pichkurov N. V.* e^+e^- Pair Production in Fast Nucleus–Heavy Atom Collision // Sov. J. Nucl. Phys. 1982. V. 35. P. 561 (Yad. Fiz. 1983. V. 35. P. 964).

29. *Baier V. N., Fadin V. S.* Pair Electroproduction Processes in Colliding-Beam Experiments // Pis'ma Zh. Eksp. Teor. Fiz. 1971. V. 13. P. 239.

30. *Ivanov D. et al.* Production of e^+e^- Pairs to All Orders in Z Alpha for Collisions of High-Energy Muons with Heavy Nuclei // Phys. Lett. B. 1998. V. 442. P. 453.

31. *Adamyan F. et al.* Experimental Study of Photon Beam Polarimeter Based on Nuclear e^+e^- Pair Production in an Amorphous Target // Nucl. Instr. Meth. A. 2007. V. 579. P. 973 and referencess therein.

32. *McKinley W. A., Feshbach H.* The Coulomb Scattering of Relativistic Electrons by Nuclei // Phys. Rev. 1948. V. 74. P. 1759;
Dalitz R. H. On Higher Born Approximations in Potential Scattering // Proc. Roy. Soc. (London). 1951. V. 206. P. 509.

33. *Baier V., Katkov V.* Corrections to Eikonal Approximation and Bremsstrahlung of Electrons at High Energy // Sov. Phys. Dokl. 1976. V. 21. P. 150 (Dokl. Akad. Nauk SSSR. 1976. V. 227. P. 325).

34. *Bazhanov V. V. et al.* Small Angle Scattering in Quantum Electrodynamics // Theor. Math. Phys. 1978. V. 33. P. 982 (Teor. Mat. Fiz. 1977. V. 33. P. 218);
Solovev L. D., Yushin Yu. Y. Investigation of Infrared Singularities in Quantum Electrodynamics by the Feynman Diagram Method // Teor. Mat. Fiz. 1978. V. 36. P. 3.

35. *Hencken K., Trautmann D., Baur G.* // Phys. Rev. A. 1995. V. 51. P. 1874; nucl-th/9410014.

36. *Baur G.* Multiple Electron Positron Pair Production in Relativistic Heavy Ion Collisions: A Strong Field Effect // Phys. Rev. A. 1990. V. 42. P. 5736.

37. *Lee R. N., Milstein A. I., Serbo V. G.* Structure of the Coulomb and Unitarity Corrections to the Cross-Section of e^+e^- Pair Production in Ultrarelativistic Nuclear Collisions // Phys. Rev. A. 2002. V. 65. P. 022102; hep-ph/0108014.

38. *Bartos E.* The Lepton Pair Production in Heavy Ion Collisions Revisited // Phys. Rev. A. 2002. V. 66. P. 042720; hep-ph/0109281.

39. *Abramovsky V. A., Gribov V. N., Kancheli O. V.* Character of Inclusive Spectra and Fluctuations Produced in Inelastic Process by Multipomeron Exchange // Yad. Fiz. 1973. V. 18. P. 595 (Sov. J. Nucl. Phys. 1974. V. 18. P. 308).

40. *Gluckstern R. L., Hull M. H.* Polarization Dependence of the Integrated Bremsstrahlung Cross Section // Phys. Rev. 1953. V. 90. P. 1030.

41. *Motz J. W., Olsen H. A., Koch H. W.* Pair Production by Photons // Rev. Mod. Phys. 1969. V. 41. P. 581.

42. *Mork K., Olsen H.* Radiative Corrections: 1. High-Energy Bremsstrahlung and Pair Production // Phys. Rev. B. 1965. V. 140. P. B1661.